

AperTO - Archivio Istituzionale Open Access dell'Università di Torino

## Modeling the avoidance behavior of zooplankton on phytoplankton infected by free viruses

### **This is the author's manuscript**

*Original Citation:*

*Availability:*

This version is available <http://hdl.handle.net/2318/1743424> since 2020-07-08T15:53:46Z

*Published version:*

DOI:10.1007/s10867-020-09538-5

*Terms of use:*

Open Access

Anyone can freely access the full text of works made available as "Open Access". Works made available under a Creative Commons license can be used according to the terms and conditions of said license. Use of all other works requires consent of the right holder (author or publisher) if not exempted from copyright protection by the applicable law.

(Article begins on next page)

1 Saswati Biswas · Pankaj Kumar Tiwari · Francesca

2 Bona · Samares Pal · Ezio Venturino

# 3 Modeling the avoidance behavior of zooplankton on 4 phytoplankton infected by free viruses

5 the date of receipt and acceptance should be inserted later

6 **Abstract** In any ecosystem, chaotic situations may arise from equilibrium state for different reasons.  
7 To overcome these chaotic situations sometimes the system itself exhibits some mechanisms of self-  
8 adaptability. In this paper, we explore an eco-epidemiological model consisting of three aquatic groups:  
9 phytoplankton, zooplankton and marine free viruses. We assume that the phytoplankton population  
10 are infected by external free viruses and zooplankton get affected on consumption of infected phyto-  
11 plankton; also the infected phytoplankton do not compete for resources with the susceptible one. In  
12 addition, we model a mechanism by which zooplankton recognize and avoid infected phytoplankton,  
13 at least when susceptible phytoplankton are present. The zooplankton extinction chance increases on  
14 increasing the force of infection or decreasing the intensity of avoidance. Further, when the viral infec-  
15 tion triggers chaotic dynamics, high zooplankton avoidance intensity can stabilize again the system.  
16 Interestingly, for high avoidance intensity, nutrient enrichment has a destabilizing effect on the system  
17 dynamics, which is in line with the *paradox of enrichment*. Global sensitivity analysis helps to identify  
18 the most significant parameters that reduce the infected phytoplankton in the system. Finally, we

---

Saswati Biswas · Pankaj Kumar Tiwari · Samares Pal

Department of Mathematics, University of Kalyani, Kalyani - 741235, India

Francesca Bona

DBIOS, University of Turin, via Accademia Albertina 13, 10123 Turin, Italy

Ezio Venturino

Dipartimento di Matematica “Giuseppe Peano”, via Carlo Alberto 10, 10123 Torino, Università di Torino,  
Italy; Member of the INdAM research group GNCS

E-mail: ezio.venturino@unito.it

19 compare the dynamics of the system by allowing the infected phytoplankton also to share resources  
20 with the susceptible phytoplankton. A gradual increase of the virus replication factor turns the system  
21 dynamics from chaos to doubling state to limit cycle to stable and the system finally settles down to  
22 the zooplankton-free equilibrium point. Moreover, on increasing the intensity of avoidance, the system  
23 shows a transcritical bifurcation from the zooplankton-free equilibrium to the coexistence steady state,  
24 and remains stable thereafter.

25 **Keywords** Phytoplankton · Zooplankton · Free-virus · Avoidance behavior · Chaos · Global  
26 sensitivity.

## 27 1 Introduction

28 Phytoplankton lie at the bottom of the aquatic trophic chains. Due to presence of chlorophyll pigment  
29 in the cells, phytoplankton grow photoautotrophically in aquatic environments [1]. These unicellular  
30 organisms are basically the energy sources, from which energy flows along the food webs up to the  
31 higher trophic levels. Any potential changes in these primary producers can therefore affect the en-  
32 tire food chain structure. Marine viruses have been recognized to play a major role in altering the  
33 metabolic capacity as well as the biochemical compositions of their algal hosts [2–6]. Moreover, many  
34 studies have illustrated the ecological importance of marine viruses as agents causing mortality in ma-  
35 rine phytoplankton communities [7–11]. In the last few decades, worldwide attention has been drawn  
36 towards the impacts of diseases in ecological systems [12, 13]; in particular, algal-virus correlations and  
37 their effects on interspecies competition as well as on environmental issues [14, 15].

38 Marine viruses are exceptionally abundant, highly host-specific and have the feature of possibly  
39 infect the algae. There are two predominant ways for viral replication: the lytic and lysogenic cycle.  
40 Most of the non-enveloped and few enveloped marine viruses replicate through lytic cycles. Namely,  
41 virus particles get attached to their algal host cells and inject genome into the cell. Virus replication is  
42 performed using the hosts genetic machinery. After the completion of replication, the cell wall breaks  
43 and progeny virions are released into the environment. Viral infection alters the size, nutritional value  
44 and cell lipid membrane characteristics of the host cells. It also directly impacts on the grazing behavior  
45 and growth rate of zooplankton [16, 17]. The coccolithophores *Emiliania huxleyi* are frequently found  
46 to be one of the dominant phytoplankton species in many pelagic ecosystems. In favourable water  
47 conditions, *E. huxleyi* can grow extremely rapidly and it forms very extensive blooms especially at high  
48 latitude [18]. It is well documented that *E. huxleyi* blooms are exterminated by viral lysis, with the

49 viruses unambiguously identified as EhV [19]. During viral infection *E. huxleyi* experiences remarkable  
50 structural, biochemical and physiological changes [5, 20, 21], which in turn affect the herbivory grazing.

51 In the normal bloom conditions when viral infection has not yet started, the primary consumers  
52 like copepods, randomly feed on *E. huxleyi* and other phytoplankton species. In the presence of viral  
53 infection, however, zooplankton exhibit some grazing selection. Some zooplankton (e.g. *Acartia tonsa*)  
54 tend to avoid infected *E. huxleyi* cells in response to the chemicals released by the infected cell through  
55 their surface [18, 20]. Under stress (i.e., in the presence of grazers) algal cells liberate a moderate amount  
56 of chemicals such as dimethyl sulfide (DMS) and amino acids [22–25], which give signals to their grazers.  
57 Feeding on them will be poisonous to the grazers, so they prefer to avoid them. But during viral infection  
58 the DMS release increases considerably and becomes toxic [26, 27]. In such conditions, *Acartia tonsa*  
59 preferably ingests less infected than uninfected *E. huxleyi* cells. A further effect of consumed high  
60 lyase *E. huxleyi* cells is the increase of zooplankton mortality, caused by the reaction of the produced  
61 dimethyl gas and of the *E. huxleyi*'s calcium carbonate cell with the zooplankton's internal pH, with  
62 the consequent destruction of the latter [28].

63 Predator-prey systems with viral infection affecting the prey have been considered in [29–32], while  
64 the role of viral infection in the marine trophic chains has been investigated more specifically in [33–36].  
65 In [37] viral infection as a cause of recurrent phytoplankton blooms has been analyzed by formulating  
66 a three-species model consisting of susceptible and infected phytoplankton and their potential grazer.  
67 A virally infected phytoplankton-zooplankton system considering both susceptible and infected phy-  
68 toplankton being able to release toxic substances appears in [38]. The viral infection and “allelopathic  
69 agents” are shown to possess a major role for the control of phytoplankton blooms. The dynamics of  
70 ecological interactions caused by the infected phytoplankton where the disease is transmitted through  
71 contact have been investigated for instance in [39–42], while other models have been formulated to take  
72 into account that the disease is transmitted also through vectors or directly from the environment,  
73 e.g., pollutants, toxicant, free viruses etc., [14, 15], with the typical assumption that both the healthy  
74 and infected phytoplankton are equally likely to predation and infected phytoplankton has no negative  
75 impact on the growth of zooplankton.

76 Ecological systems possess all the elements to produce chaotic dynamics [43]. Although chaos is  
77 commonly predicted by mathematical models, evidence for its existence in the natural world is scarce  
78 and inconclusive. Even the characteristics of chaos and its presence in nature are much discussed in  
79 ecology [44–47]. Recent developments in dynamical system theory consider chaotic fluctuations of a

---

80 dynamical system as highly desirable because fluctuations allow such a system to be easily controlled.  
81 To assess the ecological implications of chaotic dynamics in different natural systems, it is important to  
82 explore changes in the dynamics when structural assumptions of the system are varied. One approach  
83 to the study of the dynamics of ecological community is via its food web and the coupling of interacting  
84 species with each other. Hastings and Powell [48] produced chaos in a three species food chain model  
85 with Holling type II functional responses. Chattopadhyay and Sarkar [49] modified the Hastings and  
86 Powell [48] model by introducing toxin producing parameter and its negative effect on zooplankton  
87 grazing on phytoplankton. Jørgensen [47] showed that chaos may appear in the planktonic system due  
88 to size variation in zooplankton species. According to the allometric principle of Peters [50], all the  
89 parameters vary as functions of size. Mandal et al. [51] applied thermodynamic principle (exergy) in  
90 the Hastings and Powell's model of phytoplankton, zooplankton and fish, showing that on gradually  
91 decreasing the zooplankton size the model dynamics changes from an equilibrium state to chaotic  
92 conditions.

93 In the present investigation, the key contribution is represented by the modeling of grazer zoo-  
94 plankton avoidance of virally infected phytoplankton in the presence of susceptible phytoplankton  
95 [17]. The variation in the zooplankton's avoidance degree of infected phytoplankton when the sus-  
96 ceptible phytoplankton levels change may have a relevant impact for the species survival and for the  
97 understanding of the internal system dynamics. The previous related model of [52] dealing with the  
98 avoidance phenomenon in the presence of toxic phytoplankton, showed that the strength of avoidance  
99 deeply influences the dominance of the toxic species. In contrast to the other former studies [14, 15], a  
100 negative effect of infected cell consumption on zooplankton, arising from the toxic chemical compounds  
101 released by viral cell lysis [17, 28], is incorporated in the present model. We study the system dynam-  
102 ics in two cases: at first we assume that the infected phytoplankton do not compete with susceptible  
103 phytoplankton for resources, while in the second case, the resources are assumed to be shared by sus-  
104 ceptible and infected phytoplankton. The model contains the zooplankton feeding avoidance of infected  
105 phytoplankton as a function of the abundance of susceptible phytoplankton. Our objective is to assess  
106 whether the avoidance behavior enhances the survival and dominance of infected phytoplankton over  
107 its susceptible competitors, as well as its effect on the zooplankton. In chaotic situations, the negative  
108 effect of infected phytoplankton on zooplankton may reduce the grazing pressure of zooplankton and  
109 as a result the system may recover from chaos and return to a stable state.

110 The rest of the paper is organized as follows: in the next section, we formulate the mathematical  
 111 model incorporating the zooplankton avoidance of infected phytoplankton in the presence of the sus-  
 112 ceptible one. The mathematical analysis in Section 3 contains the analytical findings of the model;  
 113 Hopf-bifurcation analysis is performed by taking the avoidance intensity as bifurcation parameter. In  
 114 Section 4, we numerically investigate the dynamical behavior of the system for the different parame-  
 115 ters setups. In so doing we validate the criteria obtained from the mathematical analysis illustrated  
 116 in Section 3. This section also contains the investigation of the system behavior when susceptible and  
 117 infected phytoplankton compete for common resources. A final discussion concludes the paper.

## 118 2 The mathematical model

119 Viruses represent the most abundant entities in the sea and play a major role in the control of oceans  
 120 life. However, not much is known about marine viruses and their ecological role in aquatic ecosystems,  
 121 their interaction with other species, the spread of diseases and their impact on plankton blooming. We  
 122 consider an ecological system consisting of susceptible phytoplankton ( $S$ ), infected phytoplankton ( $I$ ),  
 123 zooplankton ( $Z$ ) and the free viruses in the environment causing the infection ( $V$ ) under the following  
 124 assumptions:

- 125 1. In the absence of viral disease and the grazer zooplankton, the susceptible phytoplankton grow  
 126 logistically with intrinsic growth rate  $a$  and carrying capacity  $K$ .
2. The susceptible phytoplankton  $S$ , becomes infected by direct contact with free viruses,  $V$ . This is  
 modeled via the function

$$T_0(S, V) = \frac{\beta SV}{K_1 + V}$$

127 with transmission rate  $\beta$  and half saturation constant  $K_1$  [14].

- 128 3. Zooplankton predate on both susceptible and infected phytoplankton; while they benefit the grazing  
 129 of the former [14, 15], uptake of infected phytoplankton instead inhibits them [17, 26, 27].
4. The Holling type-II functional response to the grazer zooplankton is assumed for susceptible and  
 infected phytoplankton respectively given by

$$f_S = \frac{\alpha_1 SZ}{d_1 + S}, \quad f_I = \frac{\alpha_2 IZ}{d_2 + I},$$

130 where  $d_1$  and  $d_2$  denote the half-saturation constants for the susceptible and infected phytoplankton.

- 131 5. Several experimental outcomes reveal that whenever abundance of susceptible phytoplankton is  
 132 high, zooplankton prefer to graze on susceptible phytoplankton and avoid ingesting infected species

[17]. Also, zooplankton graze on infected phytoplankton in the presence of susceptible phytoplankton. Moreover, infected phytoplankton has no significant influence on the predation of susceptible phytoplankton, but the abundance of susceptible phytoplankton greatly reduces the ingestion of infected phytoplankton.

6. To account for the fact that the presence of susceptible phytoplankton abundance greatly reduces the ingestion of infected phytoplankton, we modify the predation rate on infected phytoplankton by introducing an extra term  $\gamma S$  in the denominator of the relevant functional response as [52],

$$J_I^* = \frac{\alpha_2 IZ}{d_2 + I + \gamma S},$$

where  $\gamma$  measures the intensity of the avoidance of infected phytoplankton by zooplankton in the presence of susceptible phytoplankton.

7.  $\gamma = 0$  produces a system where zooplankton do not discriminate between susceptible and infected phytoplankton; whereas high  $\gamma$  results in a decrease in the uptake of infected phytoplankton by zooplankton in the presence of susceptible phytoplankton, although it does not affect the uptake of susceptible phytoplankton directly. Thus, higher values of  $\gamma$  result in the lesser mortality of the zooplankton due to ingestion of infected phytoplankton. Zooplankton natural mortality is taken as a linear function,  $\nu Z$ .
8. The infected phytoplankton fail to contribute in the reproduction process due to their inability to compete for resources [53,54] as the energy required for viral replication of infected phytoplankton is negligible, and they are removed by cell lysis before having the capability of reproducing [55, 56]. Further, the infected phytoplankton are assumed not to exert intraspecific pressure on the susceptible phytoplankton [37].
9. From the time of infection to its lysis, within the body of the infected phytoplankton viruses replicate. Let  $\mu$  represent the infected phytoplankton mortality rate and  $b \gg 1$  the virus replication factor, i.e., the average number of viruses released in the environment upon infected phytoplankton lysis. The decay rate of virus is assumed to be constant,  $\delta$ . The virus is removed through the infection of susceptible phytoplankton at the rate  $T_0(S, V)$ .

Based on the above assumptions, the schematic diagram for the interactions among susceptible phytoplankton, infected phytoplankton, zooplankton and free viruses is depicted in Fig. 1. Thus, we obtain

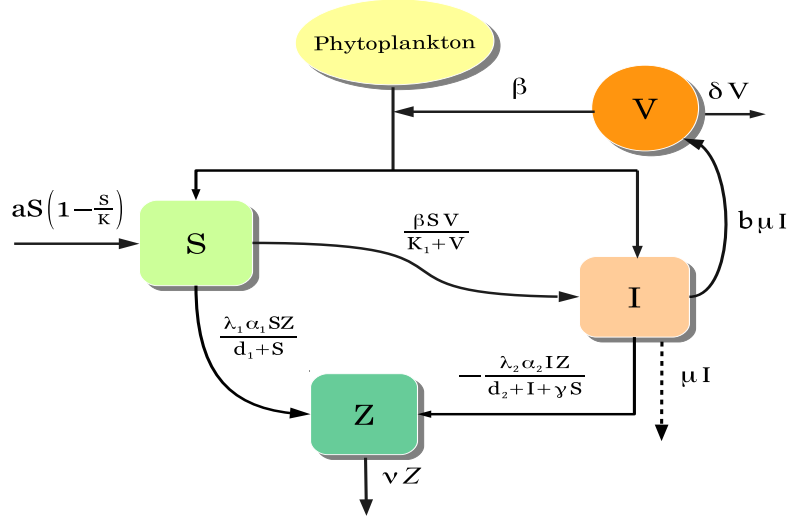


Fig. 1 Schematic diagram of system (1).

157 the following system of differential equations,

$$\begin{aligned}
 \frac{dS}{dt} &= aS \left( 1 - \frac{S}{K} \right) - \frac{\alpha_1 SZ}{d_1 + S} - \frac{\beta SV}{K_1 + V}, \\
 \frac{dI}{dt} &= \frac{\beta SV}{K_1 + V} - \frac{\alpha_2 IZ}{d_2 + I + \gamma S} - \mu I, \\
 \frac{dZ}{dt} &= \frac{\lambda_1 \alpha_1 SZ}{d_1 + S} - \frac{\lambda_2 \alpha_2 IZ}{d_2 + I + \gamma S} - \nu Z, \\
 \frac{dV}{dt} &= b\mu I - \frac{\beta SV}{K_1 + V} - \delta V.
 \end{aligned} \tag{1}$$

158 All parameters involved in the system (1) are assumed to be positive, and their biological meanings  
 159 are given in Table 1.

160

### 161 3 Mathematical Analysis

162 We first have the following theorem regarding the positivity property, boundedness and permanence  
 163 of the system (1).

164 **Theorem 1** *System (1) is positively invariant and bounded in  $R_+^4$ , and the feasible region for system*  
 165 *(1) is the following set*

$$\Omega = \left\{ (S, I, Z, V) : 0 \leq S + I + Z + \frac{\nu}{b\mu} V \leq M \right\},$$



**Table 1** The meaning of the model parameters and their hypothetical values, chosen within ranges prescribed in the literature [14,15].

Parameters	Descriptions	Values	Units
$a$	Intrinsic growth rate of susceptible phytoplankton	0.75	day <sup>-1</sup>
$K$	Carrying capacity of susceptible phytoplankton	108	cells L <sup>-1</sup>
$\alpha_1$	Consumption rate of susceptible phytoplankton by zooplankton	0.045	day <sup>-1</sup>
$d_1$	Half-saturation constant for the consumption of susceptible phytoplankton by zooplankton	2	cells L <sup>-1</sup>
$\beta$	Force of infection	0.65	day <sup>-1</sup>
$K_1$	Half-saturation constant for the infection of susceptible phytoplankton by free-viruses	3	cells L <sup>-1</sup>
$\alpha_2$	Consumption rate of infected phytoplankton by zooplankton	0.045	day <sup>-1</sup>
$d_2$	Saturation constant for the consumption of infected phytoplankton by zooplankton	2	cells L <sup>-1</sup>
$\gamma$	Intensity of avoidance	3.8	—
$\mu$	Death rate of infected phytoplankton	0.16	day <sup>-1</sup>
$\lambda_1$	Growth of zooplankton on consumption of susceptible phytoplankton	0.75	—
$\lambda_2$	Death of zooplankton on consumption of infected phytoplankton	0.61	—
$\nu$	Death rate of zooplankton	0.012	day <sup>-1</sup>
$b$	Virus replication factor	35	—
$\delta$	Decay rate of free viruses	1.23	day <sup>-1</sup>

166 which is compact and invariant with respect to system (1). Further, let the following inequalities be  
 167 satisfied, where  $S_a$ ,  $I_m$ ,  $Z_m$  and  $V_m$  are defined in the proof:

$$a > \frac{\beta V_m}{K_1} + \frac{\alpha_1 Z_m}{d_1}, \quad \beta > \frac{I_m}{S_a} \left( \frac{\alpha_2 Z_m}{d_2} + \mu \right), \quad \frac{\lambda_1 \alpha_1 S_a}{d_1 + S_a} > \nu + \frac{\lambda_2 \alpha_2 I_m}{d_2}. \quad (2)$$

168 Then the system (1) is uniformly persistent.

169 *Proof* System (1) has a Lipschitz-continuous right hand side, so that the existence and uniqueness  
 170 theorem for its solutions holds. Observe further that it is homogeneous, so that the coordinate axes  
 171 and (hyper)planes cannot be crossed, being themselves solutions. Therefore, any trajectory of the  
 172 system (1) starting from an initial state in  $\mathbb{R}_+^4$  remains trapped in  $\mathbb{R}_+^4$ .

173 We define a new variable  $U = S + I + Z + \frac{\nu}{b\mu}V$ . For an arbitrary  $\sigma > 0$ , by summing up the  
 174 equations in system (1), we find

$$\begin{aligned} \frac{dU}{dt} + \sigma U &= (a + \sigma)S - \frac{aS^2}{K} - \{(\mu - \nu) - \sigma\}I - (\nu - \sigma)Z - \frac{\nu}{b\mu}(\delta - \sigma)V - \frac{(1 - \lambda_1)\alpha_1 SZ}{d_1 + S} \\ &\quad - \frac{(1 + \lambda_2)\alpha_2 IZ}{d_2 + I + \gamma S} - \frac{\nu}{b\mu} \frac{\beta SV}{K_1 + V}. \end{aligned}$$

175 Since  $\lambda_1 \leq 1$ , after choosing  $\sigma \leq \min\{(\mu - \nu), \nu, \delta\}$ , we obtain the following upper bound:

$$\frac{dU}{dt} + \sigma U \leq (a + \sigma)S - \frac{aS^2}{K} \leq \frac{K(a + \sigma)^2}{4a} = L.$$

176 Applying standard results on differential inequalities [57], we have

$$U(t) \leq e^{-\sigma t} \left( U(0) - \frac{L}{\sigma} \right) + \frac{L}{\sigma} \leq \max \left\{ \frac{L}{\sigma}, U(0) \right\} = M.$$

177 Thus, there exists an  $M > 0$ , depending only on the system parameters, such that  $U(t) \leq M$ . Hence,  
178 the solutions of system (1) and consequently all the system populations are ultimately bounded above.

Since

$$\limsup_{t \rightarrow \infty} \left[ S(t) + I(t) + Z(t) + \frac{\nu}{b\mu} V(t) \right] \leq M$$

179 and  $\lim_{t \rightarrow \infty} S(t) \leq K$ , there exist  $T_1, T_2, T_3, T_4 > 0$  such that  $S(t) \leq K \forall t \geq T_1$ ,  $I(t) \leq I_m \forall t \geq T_2$ ,  
180  $Z(t) \leq Z_m \forall t \geq T_3$ ,  $V(t) \leq V_m$  for all  $t \geq T_4$ , where  $I_m, Z_m$  and  $V_m$  are finite positive constants with  
181  $K + I_m + Z_m + V_m \leq M$ . Hence, for all  $t \geq \max\{T_1, T_2, T_3, T_4\} = T$ ,  $S(t) \leq K$ ,  $I(t) \leq I_m$ ,  $Z(t) \leq Z_m$   
182 and  $V(t) \leq V_m$ . Let us define  $M_1 = \max\{K, I_m, Z_m, V_m\}$ .

183 Now, from the first equation of system (1), we have

$$\frac{dS}{dt} \geq aS \left( 1 - \frac{S}{K} \right) - \frac{\beta S V_m}{K_1} - \frac{\alpha_1 S Z_m}{d_1}.$$

184 Hence, it follows that for some  $S_a$ ,

$$\liminf_{t \rightarrow \infty} S(t) \geq \frac{K}{a} \left( a - \frac{\beta V_m}{K_1} - \frac{\alpha_1 Z_m}{d_1} \right) = S_a.$$

185 From the second equation of system (1), we have

$$\frac{dI}{dt} \geq \frac{\beta S_a V}{K_1 + V} - \frac{\alpha_2 Z_m I_m}{d_2} - \mu I_m > 0$$

186 provided that

$$V(t) > \frac{K_1 I_m \left( \frac{\alpha_2 Z_m}{d_2} + \mu \right)}{\beta S_a - I_m \left( \frac{\alpha_2 Z_m}{d_2} + \mu \right)}.$$

Let  $V_a > 0$  be such that

$$\frac{K_1 I_m \left( \frac{\alpha_2 Z_m}{d_2} + \mu \right)}{\beta S_a - I_m \left( \frac{\alpha_2 Z_m}{d_2} + \mu \right)} < V_a < V_m,$$

187 then  $\frac{dI}{dt} > 0$  for  $V(t) \geq V_a > 0$ , for all  $t > T$ . So, there exist  $T_5 > 0$  and  $0 < I_a < I_m$  such that  
188  $I(t) \geq I_a$  for all  $t \geq T_5$ . Therefore, for all  $t \geq \max\{T, T_5\} = T'$  if  $V_a \leq V(t) \leq V_m$ , then  $I_a \leq I(t) \leq I_m$ .

189 From the third equation of system (1), we have

$$\frac{dZ}{dt} \geq Z \left( \frac{\lambda_1 \alpha_1 S_a}{d_1 + S_a} - \frac{\lambda_2 \alpha_2 I_m}{d_2} - \nu \right).$$

190 Hence, it follows that for some  $Z_a$ ,

$$\liminf_{t \rightarrow \infty} Z(t) \geq Z(0) = Z_a$$

191 provided that

$$\frac{\lambda_1 \alpha_1 S_a}{d_1 + S_a} > \nu + \frac{\lambda_2 \alpha_2 I_m}{d_2}.$$

192 Let  $M_2 = \min\{S_a, I_a, Z_a, V_a\}$ . For  $M_2$  to be positive, conditions in (2) must hold. Hence, the theorem  
193 follows.

### 194 3.1 The ecosystem in the absence of free-viruses

195 In the absence of viral disease in phytoplankton, system (1) reduces to the following simple subsystem,

$$\begin{aligned} \frac{dS}{dt} &= aS \left( 1 - \frac{S}{K} \right) - \frac{\alpha_1 SZ}{d_1 + S}, \\ \frac{dZ}{dt} &= \frac{\lambda_1 \alpha_1 SZ}{d_1 + S} - \nu Z, \end{aligned} \quad (3)$$

196 whose dynamics have been well studied [58]. Here, we summarize its dynamics as follows. System (3)  
197 has three feasible equilibria.

- 198 1. The plankton-free equilibrium  $e_0 = (0, 0)$ , which is always a saddle.
- 199 2. If  $K(\lambda_1 \alpha_1 - \nu) < d_1 \nu$ , then the zooplankton-free equilibrium  $e_1 = (K, 0)$  is globally asymptotically  
200 stable.
3. If  $K(\lambda_1 \alpha_1 - \nu) > d_1 \nu$  and  $K < \frac{d_1(\lambda_1 \alpha_1 + \nu)}{\lambda_1 \alpha_1 - \nu}$ , then the coexistence equilibrium  $e_* = (S_*, Z_*)$  is  
globally asymptotically stable, where

$$S_* = \frac{d_1 \nu}{\lambda_1 \alpha_1 - \nu}, \quad Z_* = \frac{\lambda_1 a d_1 \{K(\lambda_1 \alpha_1 - \nu) - d_1 \nu\}}{K(\lambda_1 \alpha_1 - \nu)^2}.$$

- 201 4. If  $K(\lambda_1 \alpha_1 - \nu) > d_1 \nu$  and  $K > \frac{d_1(\lambda_1 \alpha_1 + \nu)}{\lambda_1 \alpha_1 - \nu}$ , then there is a unique globally asymptotically stable  
202 limit cycle around the coexistence equilibrium  $e_* = (S_*, Z_*)$ .

203 3.2 Equilibrium analysis of full system (1)

System (1) exhibits five non-negative equilibria, of which the origin  $E_0 = (0, 0, 0, 0)$  and the point with only susceptible phytoplankton  $E_1 = (K, 0, 0, 0)$  are always feasible. The disease-free equilibrium  $E_2 = (S_2, 0, Z_2, 0)$ , with

$$S_2 = \frac{\nu d_1}{\lambda_1 \alpha_1 - \nu}, \quad Z_2 = \frac{K(\lambda_1 \alpha_1 - \nu) - \nu d_1}{K(\lambda_1 \alpha_1 - \nu)}$$

204 is feasible provided the following inequality holds

$$K(\lambda_1 \alpha_1 - \nu) - \nu d_1 > 0. \quad (4)$$

The zooplankton-free equilibrium  $E_3 = (S_3, I_3, 0, V_3)$  has the populations

$$S_3 = \frac{K\{aK_1 + V_3(a - \beta)\}}{a(K_1 + V_3)}, \quad I_3 = \frac{K\beta V_3\{aK_1 + V_3(a - \beta)\}}{a\mu(K_1 + V_3)^2},$$

205 where  $V_3$  is a positive root of the quadratic

$$a_2 V^2 + a_1 V + a_0 = 0, \quad (5)$$

206 with coefficients

$$a_2 = a\delta, \quad a_1 = 2aK_1\delta - (b - 1)\beta K(a - \beta), \quad a_0 = aK_1[\delta K_1 - \beta K(b - 1)].$$

207 A necessary condition for feasibility is then  $S_3 \geq 0$ , which entails

$$aK_1 + V_3(a - \beta) > 0. \quad (6)$$

208 Because  $a_2 > 0$ , equation (5) has exactly one positive root if  $a_0 < 0$ . Thus, sufficient conditions for  $E_3$   
209 to be feasible are given by

$$aK_1 + V_3(a - \beta) > 0, \quad \beta K(b - 1) - \delta K_1 > 0. \quad (7)$$

210 In case the latter is not satisfied, equation (5) has either two or no positive roots.

211 Coexistence  $E^* = (S^*, I^*, Z^*, V^*)$  can be completely characterized. It has the populations:

$$Z^* = \frac{d_1 + S^*}{\alpha_1} \left[ a \left( 1 - \frac{S^*}{K} \right) - \frac{\beta V^*}{K_1 + V^*} \right], \quad I^* = F_1(S^*), \quad V^* = \frac{K_1 F_2(S^*)}{\beta - F_2(S^*)}, \quad (8)$$

212 where

$$F_1(S) = \frac{(d_2 + \gamma S)[\nu(d_1 + S) - \lambda_1 \alpha_1 S]}{\lambda_1 \alpha_1 S - (d_1 + S)(\lambda_2 \alpha_2 + \nu)} = \gamma C \frac{(S - S_{F_1}^-)(S_{F_1}^0 - S)}{S - S_{F_1}^\infty}, \quad C = \frac{\alpha_1 \lambda_1 - \nu}{\alpha_1 \lambda_1 - \alpha_2 \lambda_2 - \nu}, \quad (9)$$

$$S_{F_1}^0 = \frac{\nu d_1}{\alpha_1 \lambda_1 - \nu}, \quad S_{F_1}^- = -\frac{d_2}{\gamma} < 0, \quad S_{F_1}^\infty = \frac{d_1(\alpha_2 \lambda_2 + \nu)}{\alpha_1 \lambda_1 - \alpha_2 \lambda_2 - \nu}, \quad (10)$$

$$F_2(S) = \frac{\nu(d_1 + S) - \lambda_1 \alpha_1 S}{\nu(d_1 + S) - (\lambda_1 + \lambda_2)\alpha_1 S} \left[ a \left( 1 - \frac{S}{K} \right) - \frac{\mu \alpha_1 \lambda_2 (d_2 + \gamma S)}{\lambda_1 \alpha_1 S - (d_1 + S)(\lambda_2 \alpha_2 + \nu)} \right] \quad (11)$$

213 and  $S^*$  is positive root of the equation

$$F_1(S) = \Phi(S), \quad \Phi(S) = \frac{1}{b\mu} F_2(S) \left[ S + \delta \frac{K_1}{\beta - F_2(S)} \right]. \quad (12)$$

214 Analyzing the coefficients in  $F_1$ , by taking

$$\alpha_1 \lambda_1 \geq \alpha_2 \lambda_2 + \nu \quad (13)$$

215 it follows that  $C > 0$  and then  $0 \leq S_{F_1}^0 \leq S_{F_1}^\infty$ . Indeed the opposite case in (13) leads to  $F_1(S) < 0$  for  
 216  $S \geq 0$ , which is not feasible. Further, the case  $S_{F_1}^0 \leq 0 \leq S_{F_1}^\infty$  is impossible, giving a contradiction on  
 217 the signs of the coefficients of  $F_1$ . Finally,  $F_1(S) \geq 0$  for  $I_{F_1>0} = S_{F_1}^0 \leq S < S_{F_1}^\infty$ , which is the only  
 218 range of interest where to seek a solution of (12) in what follows.

219 We now perform the qualitative study of  $\Phi(S)$  in steps. As mentioned above, we concentrate on  
 220 the interval  $I_{F_1>0}$  in which  $F_1$  is feasible, because the solution of the intersection problem (12) must  
 221 be feasible, and therefore lie in this range.

222 First of all, we concentrate on  $F_2(S)$ . This function can be rewritten as follows:

$$F_2(S) = \frac{C}{S_{F_2}^\infty - S} \left[ a(S_{F_1}^0 - S) \left( 1 - \frac{S}{K} \right) - \mu \alpha_1 \lambda_2 F_1(S) \right] = C \frac{S_{F_1}^0 - S}{(S_{F_2}^\infty - S)(S - S_{F_1}^\infty)} \Psi(S),$$

$$S_{F_2}^\infty = \frac{\nu d_1}{\alpha_1(\lambda_1 + \lambda_2) - \nu}, \quad \Psi(S) = a \left( 1 - \frac{S}{K} \right) (S - S_{F_1}^\infty) - \mu \alpha_1 \lambda_2 (S - S_{F_1}^-) = \sum_{k=0}^2 \theta_k S^k,$$

$$\theta_2 = -\frac{a}{K} < 0, \quad \theta_1 = a \left( \frac{S_{F_1}^\infty}{K} + 1 \right) - \mu \alpha_1 \lambda_2, \quad \theta_0 = -a S_{F_1}^\infty + \mu \alpha_1 \lambda_2 S_{F_1}^- < 0.$$

223 Thus, note that in view of (13) and (9),  $0 < S_{F_2}^\infty \leq S_{F_1}^0$ . Also  $F_2(S_{F_1}^0) = 0$ , the same zero as for  $F_1(S)$ .

224 The parabola  $\Psi$  is concave and it may or may not have real roots  $\Psi^\pm$  depending on the sign of  
 225 its discriminant  $\Delta_\Psi = \theta_1^2 - 4\theta_0\theta_2$ . If  $\Delta_\Psi < 0$ , it follows  $\Psi(S) < 0$  for every  $S \in \mathbf{R}$  and consequently  
 226  $F_2(S) < 0$ . This situation is illustrated in case (Z1) below. In case the real roots  $\Psi^\pm$  exist, there are  
 227 several subcases that need to be analysed based on their location on the real axis with respect to the  
 228 three relevant fixed knots, arranged, as we know, in the following order  $0 < S_{F_2}^\infty < S_{F_1}^0 < S_{F_1}^\infty$ . To  
 229 study these various situations, the signs of  $S - S_{F_1}^\infty$ ,  $S_{F_1}^0 - S$  and  $S_{F_2}^\infty - S$  need to be considered. In the  
 230 interval  $I_{F_1>0}$ , we find  $S - S_{F_1}^\infty < 0$ ,  $S_{F_1}^0 - S < 0$  and  $S_{F_2}^\infty - S < 0$ . By coupling them with the study  
 231 of  $F_2$ , we find the following results.

232 (Z1) Here  $\Delta_\Psi < 0$  and  $\Psi(S) < 0$ , so that  $F_2(S) > 0$  for every  $S \in I_{F_1>0}$ .

233 (Z2)  $\Delta_\Psi > 0$ ;  $\Psi^\pm$  lie both to the left or both to the right of  $I_{F_1>0}$ . Then  $F_2(S) > 0$  for every  $S \in I_{F_1>0}$ .

234 (Z3)  $\Delta_\Psi > 0$ ; if  $S_{F_1}^0 < \Psi^- < \Psi^+ < S_{F_1}^\infty$ , then  $F_2(S) > 0$  for  $S_{F_1}^0 < S < \Psi^-$  and for  $\Psi^+ < S < S_{F_1}^\infty$ .

235 (Z4)  $\Delta_\Psi > 0$ ; if  $\Psi^- < S_{F_1}^0 < \Psi^+ < S_{F_1}^\infty$ , then  $F_2(S) > 0$  for  $\Psi^+ < S < S_{F_1}^\infty$ .

236 (Z5)  $\Delta_\Psi > 0$ ; if  $S_{F_1}^0 < \Psi^- < S_{F_1}^\infty < \Psi^+$ , then  $F_2(S) > 0$  for  $S_{F_1}^0 < S < \Psi^-$ .

237 (Z6)  $\Delta_\Psi > 0$ ; if  $\Psi^- < S_{F_1}^0 < S_{F_1}^\infty < \Psi^+$ , then  $F_2(S) < 0$  for every  $S \in I_{F_1>0}$  and consequently from (12)  
 238 also  $\Phi(S) < 0$  so that no feasible intersection can exist.

239 We now examine the possibility of solving (12) in the feasible range  $I_{F_1>0}$ , for each case. Note that  
 240  $F_2$  has the same zero  $S_{F_1}^0$  of  $F_1$  and contains in its definition the latter function, so that it inherits its  
 241 vertical asymptote too,  $S_{F_1}^\infty$ .

(Z1)<sub>2</sub> (Z2) In this situation  $F_2(S) > 0$  for every  $S \in I_{F_1>0}$ . In view of the above remarks, its graph must raise up  
 243 from  $(S_{F_1}^0, 0)$  to infinity as  $S$  approaches from the left  $S_{F_1}^\infty$ . Note then that  $Y = \beta$  always intersects  
 244 the graph of  $F_2$ . We now construct the function  $\Phi$  in steps. The function  $\tilde{H}(S) = \beta - F_2(S)$  is  
 245 positive for  $S_{F_1}^0 < S \leq A^+$  where it is zero. Then  $\tilde{H}(S) = [\hat{H}(S)]^{-1}$  is positive in the same interval,  
 246 but has a vertical asymptote at  $S = A^+$  and negative in  $(A^+, S_{F_1}^\infty]$ , at which point it has a zero.  
 247 Thus  $H(S) = S + \hat{H}(S)$  is nonnegative in  $\{[S_{F_1}^0, A^+]\} \cup \{[H^+, S_{F_1}^\infty]\}$  where  $H^+$  denotes a zero of  
 248  $H(S)$ . Finally  $\Phi(S) = (b\mu)^{-1}F_2(S)H(S)$  has zeros at  $S_{F_1}^0$  and  $H^+$  and from each one of these points  
 249 on the  $S$  axis, a branch emanates raising up to infinity, the former (i) at  $A^+$  and the second one (ii)  
 250 at  $S_{F_1}^\infty$ . Comparing this behavior with the one of  $F_1(S)$  described formerly, the intersection with  
 251 the branch (ii) may not always exists, as the  $F_2$  and  $F_1$  are asymptotic to each other; indeed they  
 252 have the same vertical asymptote there. Another one might occur with branch (i), if the following  
 253 sufficient condition on the slopes of the two functions is guaranteed, so that the functions interlace,  
 254 namely

$$F_1'(S_{F_1}^0) > \Phi'(S_{F_1}^0). \quad (14)$$

255 (Z3) This case gives rise to two subcases, as  $F_2$  has one positive hump connecting the points  $(S_{F_1}^0, 0)$   
 256 and  $(\Psi^-, 0)$  and the branch tending to the vertical asymptote at  $S_{F_1}^\infty$  from  $(\Psi^+, 0)$ , depending on  
 257 whether  $Y = \beta$  intersects or not the hump of  $F_2$ .

258 (Z3a)  $Y = \beta$  has three intersections with  $F_2$ , with abscissae  $A^-, A^0, A^+$ . Then  $\tilde{H}(S) = \beta - F_2(S)$  has  
 259 zeros at these points and is positive in  $[S_{F_1}^0, A^-]$  and in  $[A^0, A^+]$ . Both  $\hat{H}(S)$  and  $H(S)$  have  
 260 asymptotes at  $A^-, A^0$  and  $A^+$ , as well as the resulting  $\Phi(S)$ , which is nonnegative in each one of  
 261 the following intervals:  $[S_{F_1}^0, A^-]$ ,  $[A^0, H^-]$ ,  $[H^+, A^+]$ ,  $[A^*, S_{F_1}^\infty]$ . Thus  $\Phi$  has four branches that  
 262 either raise up to or come down from infinity and join the points on the  $S$  axis with abscissae  
 263  $S_{F_1}^0, H^-, H^+, A^*$ . Thus  $F_1$  is bound to intersect the two intermediate of them, is asymptotic  
 264 to the rightmost one, and might intersect the leftmost one if the condition (14) holds.

(Z3b) In this subcase only one intersection of  $Y = \beta$  with  $F_2$  exists, giving rise to the zero  $A^+$  of  $\tilde{\Pi}$ . The latter function is positive for  $S_{F_1}^0 \leq S \leq S^+$ ,  $\hat{\Pi}$ ,  $\Pi$  and  $\Phi$  possess a vertical asymptote at  $S = A^+$ . Thus  $\Pi$  is nonnegative in the intervals  $[S_{F_1}^0, A^-]$ ,  $[A^0, \Pi^-]$ ,  $[\Pi^+, A^+)$ ,  $[A^*, S_{F_1}^\infty)$ . Comparing with  $F_1$  an intersection occurs with the branch lying in  $[\Pi^+, A^+)$  and a second one might occur in the first interval  $[S_{F_1}^0, A^-]$  if the slope of  $F_1$  in this case is small enough, precisely if

$$F_1'(S_{F_1}^0) < \Phi'(S_{F_1}^0). \quad (15)$$

(Z4) The function  $F_2$  is intercepted by  $Y = \beta$  only once, as it possesses only one nonnegative branch in  $[\Psi^+, S_{F_1}^\infty)$ . It follows that  $\tilde{\Pi}$  is nonnegative in  $[S_{F_1}^0, A^+]$ ,  $\hat{\Pi}$  is also, but has a vertical asymptote at  $S = A^+$ , the same occurs for  $\Pi$ , which is nonnegative also in  $[\Pi^+, S_{F_1}^\infty)$ . As a consequence,  $\Phi$  has two branches raising up to the vertical asymptotes from the points of abscissa  $\Psi^+$  and  $\Pi^+$ . An intersection of  $F_1$  is thus guaranteed with the leftmost branch.

(Z5) In this case the nonnegative part of the function  $F_2$  is a hump joining the points on the  $S$  axis with abscissae  $S_{F_1}^0$  and  $\Psi^-$ . Again two subcases arise, whether  $Y = \beta$  does or does not intercept this hump.

(Z5a) Two intersections of  $Y = \beta$  with  $F_2$  must occur with abscissae within  $[S_{F_1}^0, \Psi^-]$ . Then  $\tilde{\Pi}$  is nonnegative in  $[S_{F_1}^0, A^-]$  and  $[A^+, S_{F_1}^\infty)$  and similarly for  $\hat{\Pi}$ , but for the fact that at  $A^-$  and  $A^+$  vertical asymptotes occur and at  $S_{F_1}^\infty$  there is a zero. For  $\Pi$  similar properties hold, but for the latter, and finally  $\Phi$  results nonnegative in  $[S_{F_1}^0, A^-]$  and in  $[A^+, \Psi^-]$ . The intersection with  $F_1$  exists always in this latter interval, and one further can occur in the former, if the condition (14) is satisfied.

(Z5b) If  $Y = \beta$  lies entirely above  $F_2$ ,  $\tilde{\Pi} > 0$  on the whole  $I_{F_1} > 0$ ,  $\hat{\Pi} \geq 0$  in it, with  $\hat{\Pi}(S_{F_1}^\infty) = 0$ ,  $\Pi$  shares the same property and moreover  $\Pi(S_{F_1}^0) = \Pi(S_{F_1}^\infty) = S_{F_1}^\infty + \beta^{-1}$ , and finally  $\Phi$  has a nonnegative hump exactly in the same interval where  $F_2$  does,  $[S_{F_1}^0, \Psi^-]$ . To have an intercept with  $F_1$  we must once more require the slope condition (15).

Note that the conditions (14) and (15) can be explicitly evaluated, and namely simplify to

$$F_1'(S_{F_1}^0) = \gamma C \frac{S_{F_1}^0 - S_{F_1}^-}{S_{F_1}^\infty - S_{F_1}^0}, \quad \Phi'(S_{F_1}^0) = \frac{1}{b\mu} F_2'(S_{F_1}^0) \left( S_{F_1}^0 + \frac{K_1 \delta}{\beta} \right), \quad F_2'(S_{F_1}^0) = -C \Phi(S_{F_1}^0). \quad (16)$$

290 3.3 Stability analysis

291 The Jacobian  $J$  of system (1) has three vanishing entries, namely  $J_{12} = J_{34} = J_{43} = 0$ . The other  
292 components are

$$\begin{aligned} J_{11} &= a \left( 1 - \frac{2S}{K} \right) - \frac{d_1 \alpha_1 Z}{(d_1 + S)^2} - \frac{\beta V}{K_1 + V}, \quad J_{13} = -\frac{\alpha_1 S}{d_1 + S}, \quad J_{14} = -\frac{K_1 \beta S}{(K_1 + V)^2}, \\ J_{21} &= \frac{\beta V}{K_1 + V} + \frac{\alpha_2 \gamma I Z}{(d_2 + I + \gamma S)^2}, \quad J_{22} = -\frac{\alpha_2 Z (d_2 + \gamma S)}{(d_2 + I + \gamma S)^2} - \mu, \quad J_{23} = -\frac{\alpha_2 I}{d_2 + I + \gamma S}, \\ J_{24} &= \frac{K_1 \beta S}{(K_1 + V)^2}, \quad J_{31} = \frac{\lambda_1 d_1 \alpha_1 Z}{(d_1 + S)^2} + \frac{\lambda_2 \alpha_2 \gamma I Z}{(d_2 + I + \gamma S)^2}, \quad J_{32} = -\frac{\lambda_2 \alpha_2 Z (d_2 + \gamma S)}{(d_2 + I + \gamma S)^2}, \\ J_{33} &= \frac{\lambda_1 \alpha_1 S}{d_1 + S} - \frac{\lambda_2 \alpha_2 I}{d_2 + I + \gamma S} - \nu, \quad J_{41} = -\frac{\beta V}{K_1 + V}, \quad J_{42} = b\mu, \quad J_{44} = -\left( \delta + \frac{K_1 \beta S}{(K_1 + V)^2} \right). \end{aligned}$$

The origin  $E_0$  is unstable, having the eigenvalues  $a > 0$ ,  $-\mu$ ,  $-\nu$  and  $-\delta$ . Two eigenvalues factorize in the case of  $E_1$ ,

$$-a < 0, \quad \frac{\lambda_1 \alpha_1 K}{d_1 + K} - \nu,$$

and the Routh-Hurwitz conditions on the remaining minor become

$$\frac{\beta K}{K_1} + \delta + \mu > 0, \quad \mu \left( \delta - \frac{(b-1)\beta K}{K_1} \right) > 0.$$

293 Stability thus holds if the following conditions are satisfied:

$$\delta K_1 - \beta(b-1)K > 0, \quad \nu d_1 - K(\lambda_1 \alpha_1 - \nu) > 0. \quad (17)$$

294 At  $E_2$  the characteristic equation factorizes into the product of two quadratic equations,

$$\rho^2 + C_1 \rho + C_2 = 0, \quad \rho^2 + C_3 \rho + C_4 = 0, \quad (18)$$

295 with  $C_1 = J_{22}(E_2) + J_{44}(E_2) > 0$ ,  $C_2 = J_{22}(E_2)J_{44}(E_2) - J_{14}(E_2)J_{42}(E_2)$ ,  $C_3 = -J_{11}(E_2)$ ,  $C_4 =$   
296  $J_{13}(E_2)J_{31}(E_2) > 0$ , because the Jacobian entries simplify as follows:

$$\begin{aligned} J_{11}(E_2) &= \frac{aS_2}{K} - \frac{\alpha_1 S_2 Z_2}{(d_1 + S_2)^2}, \quad J_{13}(E_2) = \frac{\alpha_1 S_2}{d_1 + S_2}, \quad J_{14}(E_2) = J_{24} = \frac{\beta S_2}{K_1}, \quad J_{42}(E_2) = b\mu, \\ J_{22}(E_2) &= \frac{\alpha_2 Z_2}{d_2 + \gamma S_2} + \mu, \quad J_{31}(E_2) = \frac{\lambda_1 d_1 \alpha_1 Z_2}{(d_1 + S_2)^2}, \quad J_{32}(E_2) = \frac{\lambda_2 \alpha_2 Z_2}{d_2 + \gamma S_2}, \quad J_{44}(E_2) = \frac{\beta S_2}{K_1} + \delta. \end{aligned}$$

297 In view of  $C_1 > 0$  and  $C_4 > 0$ , all roots of the equations in (18) are either negative or have negative  
298 real parts if and only if  $C_2$  and  $C_3$  are positive. Thus, the equilibrium  $E_2$  is locally asymptotically  
299 stable provided

$$\delta \left( \frac{\alpha_2 Z_2}{d_2 + \gamma S_2} + \mu \right) + \frac{\beta S_2}{K_1} \frac{\alpha_2 Z_2}{d_2 + \gamma S_2} - \frac{\mu(b-1)\beta S_2}{K_1} > 0, \quad a(d_1 + S_2)^2 > K\alpha_1 Z_2. \quad (19)$$



300 One eigenvalue of the Jacobian  $J(E_3)$  factorizes to provide the necessary stability condition

$$\frac{\lambda_1 \alpha_1 S_3}{d_1 + S_3} < \frac{\lambda_2 \alpha_2 I_3}{d_2 + I_3 + \gamma S_3} + \nu \quad (20)$$

301 and other three are given by roots of the cubic

$$\rho^3 + B_1 \rho^2 + B_2 \rho + B_3 = 0, \quad (21)$$

302 where

$$B_1 = J_{11}(E_3) + J_{22}(E_3) + J_{44}(E_3),$$

$$B_2 = J_{11}(E_3)J_{22}(E_3) + J_{11}(E_3)J_{44}(E_3) + J_{22}(E_3)J_{44}(E_3) - J_{14}(E_3)J_{42}(E_3) - J_{14}(E_3)J_{21}(E_3),$$

$$B_3 = J_{11}(E_3)J_{22}(E_3)J_{44}(E_3) - J_{11}(E_3)J_{14}(E_3)J_{42}(E_3) + J_{14}(E_3)J_{21}(E_3)J_{42}(E_3) - J_{14}(E_3)J_{21}(E_3)J_{22}(E_3)$$

303 with

$$J_{11}(E_3) = \frac{aS_3}{K}, \quad J_{13}(E_3) = \frac{\alpha_1 S_3}{d_1 + S_3}, \quad J_{14}(E_3) = J_{24}(E_3) = \frac{K_1 \beta S_3}{(K_1 + V_3)^2},$$

$$J_{21}(E_3) = J_{41}(E_3) = \frac{\beta V_3}{K_1 + V_3}, \quad J_{22} = \mu, \quad J_{23}(E_3) = \frac{\alpha_2 I_3}{d_2 + I_3 + \gamma S_3},$$

$$J_{33}(E_3) = \frac{\lambda_1 \alpha_1 S_3}{d_1 + S_3} - \frac{\lambda_2 \alpha_2 I_3}{d_2 + I_3 + \gamma S_3} - \nu, \quad J_{42}(E_3) = b\mu, \quad J_{44}(E_3) = \frac{K_1 \beta S_3}{(K_1 + V_3)^2} + \delta.$$

304 The roots of equation (21) are either negative or with negative real parts if and only if the Routh-  
305 Hurwitz conditions criterion are satisfied,

$$B_1 > 0, \quad B_3 > 0, \quad B_1 B_2 - B_3 > 0, \quad (22)$$

306 so that in such case and if (20) holds,  $E_3$  is locally asymptotically stable.

307 At coexistence, note that the Jacobian has only one simplification, namely  $J_{33}(E^*) = J_{33}^* = 0$ . The  
308 associated characteristic equation is

$$\rho^4 + \sigma_1 \rho^3 + \sigma_2 \rho^2 + \sigma_3 \rho + \sigma_4 = 0, \quad (23)$$

309 where

$$\sigma_1 = J_{11}^* + J_{22}^* + J_{44}^*,$$

$$\sigma_2 = J_{11}^* J_{22}^* + J_{11}^* J_{44}^* + J_{13}^* J_{31}^* - J_{14}^* J_{41}^* + J_{22}^* J_{44}^* - J_{23}^* J_{32}^* - J_{24}^* J_{42}^*,$$

$$\sigma_3 = J_{11}^* J_{22}^* J_{44}^* - J_{11}^* J_{23}^* J_{32}^* - J_{11}^* J_{24}^* J_{42}^* + J_{13}^* J_{31}^* J_{22}^* + J_{13}^* J_{31}^* J_{44}^* \\ - J_{13}^* J_{21}^* J_{32}^* + J_{14}^* J_{21}^* J_{42}^* - J_{14}^* J_{22}^* J_{41}^* - J_{23}^* J_{32}^* J_{44}^*,$$

$$\sigma_4 = J_{13}^* J_{22}^* J_{31}^* J_{44}^* - J_{11}^* J_{23}^* J_{32}^* J_{44}^* - J_{13}^* J_{21}^* J_{32}^* J_{44}^* - J_{13}^* J_{24}^* J_{31}^* J_{42}^* \\ + J_{13}^* J_{24}^* J_{32}^* J_{41}^* - J_{14}^* J_{23}^* J_{31}^* J_{42}^* + J_{14}^* J_{23}^* J_{32}^* J_{41}^*.$$

310 Again using the Routh-Hurwitz criterion,  $E^*$ , whenever feasible, is locally asymptotically stable if and  
 311 only if the following conditions are satisfied,

$$\sigma_1 > 0, \sigma_4 > 0, \sigma_1\sigma_2 - \sigma_3 > 0, \sigma_3(\sigma_1\sigma_2 - \sigma_3) - \sigma_1^2\sigma_4 > 0. \quad (24)$$

312 In summary, we have the following theorem.

313 **Theorem 2** *The origin  $E_0$  is always unstable. The phytoplankton only equilibrium  $E_1$  is stable pro-*  
 314 *vided condition (17) holds. The disease-free equilibrium  $E_2$ , if feasible, is stable if the conditions in*  
 315 *(19) hold. The zooplankton-free equilibrium  $E_3$ , if feasible, is stable if conditions (20) and (22) hold.*  
 316 *The coexistence equilibrium  $E^*$ , if feasible, is stable if the conditions in (24) hold.*

### 317 3.4 Nonexistence of periodic solutions

318 Periodic solutions can be ruled out using the approach of [59]. We have the following result.

319 **Theorem 3** *The system (1) has no periodic solution around the interior equilibrium  $E^*$  if*

$$\begin{aligned} a + \alpha_1 + \frac{K_1\beta S^*}{(K_1 + V^*)^2} + b\mu + \frac{\alpha_1 S^*}{d_1 + S^*} + \frac{\beta V^*}{K_1 + V^*} + \frac{\alpha_2 I^*}{d_2 + I^* + \gamma S^*} + \frac{\lambda_2 \alpha_2 \{d_2 + \gamma(S^* + I^*)\} Z^*}{(d_2 + I^* + \gamma S^*)^2} \\ + \frac{\lambda_1 \alpha_1 d_1 Z^*}{(d_1 + S^*)^2} < \min \left\{ \beta + \mu + \frac{\alpha_1 Z^*}{d_1} + \frac{2aS^*}{K} + \frac{\alpha_2 Z^*}{d_2 + \gamma S^*}, \mu + \frac{\alpha_2 Z^*}{d_2 + \gamma S^*}, \beta + \frac{\alpha_1 Z^*}{d_1} + \frac{2aS^*}{K}, \right. \\ \left. \beta \left( 1 + \frac{S^*}{K_1} \right) + \delta + \frac{2aS^*}{K} + \frac{\alpha_1 Z^*}{d_1}, \mu + \delta + \frac{\beta S^*}{K_1} + \frac{\alpha_2 Z^*}{d_2 + \gamma S^*}, \delta + \frac{\beta S^*}{K_1} \right\}. \quad (25) \end{aligned}$$

320 *Proof* The second additive compound matrix of the Jacobian of the system (1) is given by

$$J^{[2]} = \begin{pmatrix} F_S + G_I & G_Z & G_V & -F_Z & -F_V & 0 \\ H_I & F_S & 0 & 0 & 0 & -F_V \\ L_I & 0 & F_S + L_V & 0 & 0 & F_Z \\ -H_S & G_S & 0 & G_I & 0 & -G_V \\ -L_S & 0 & G_S & 0 & G_I + L_V & G_Z \\ 0 & -L_S & H_S & -L_I & H_I & L_V \end{pmatrix},$$

321 where

$$F_S = -J_{11}^*, F_Z = -J_{13}^*, F_V = -J_{14}^*, G_S = J_{21}^*, G_I = -J_{22}^*, G_Z = -J_{23}^*,$$

$$G_V = J_{24}^*, H_S = J_{31}^*, H_I = -J_{32}^*, L_S = -J_{41}^*, L_I = J_{42}^*, L_V = -J_{44}^*.$$

Let  $|X|_\infty = \sup_i |X_i|$ . The logarithmic norm  $\mu_\infty(J^{[2]})$  of  $J^{[2]}$  endowed with the vector norm  $|X|_\infty$  is the supremum of  $F_S + G_I + |G_Z| + |G_V| + |F_Z| + |F_V|$ ,  $|H_I| + F_S + |F_V|$ ,  $|L_I| + F_S + L_V + |F_Z|$ ,  $|H_S| + |G_S| + G_I + |G_V|$ ,  $|L_S| + |G_S| + G_I + L_V + |G_Z|$  and  $|L_S| + |H_S| + |L_I| + |H_I| + |L_V|$ .

Now,  $(F_S + G_I + |G_Z| + |G_V| + |F_Z| + |F_V|)_{E^*} < 0$  if

$$a + \alpha_1 + \frac{K_1\beta S^*}{(K_1 + V^*)^2} + \frac{\alpha_2 I^*}{d_2 + I^* + \gamma S^*} < \beta + \frac{2aS^*}{K} + \mu + \frac{\alpha_1 Z^*}{d_1} + \frac{\alpha_2 Z^*}{d_2 + \gamma S^*};$$

similarly  $(|H_S| + F_S + |F_V|)_{E^*} < 0$  if

$$a + \frac{K_1\beta S^*}{(K_1 + V^*)^2} + \frac{\lambda_2 \alpha_2 (d_2 + \gamma S^*) Z^*}{(d_2 + I^* + \gamma S^*)^2} < \frac{2aS^*}{K} + \beta + \frac{\alpha_1 Z^*}{d_1};$$

also,  $(|L_I| + F_S + L_V + |F_Z|)_{E^*} < 0$  if

$$a + b\mu + \frac{\alpha_1 S^*}{d_1 + S^*} < \beta + \delta + \frac{2aS^*}{K} + \frac{\alpha_1 Z^*}{d_1} + \frac{\beta S^*}{K_1};$$

further  $(|H_S| + |G_S| + G_I + |G_V|)_{E^*} < 0$  if

$$\frac{\lambda_1 \alpha_1 d_1 Z^*}{(d_1 + S^*)^2} + \frac{\alpha_2 \gamma I^* Z^*}{(d_2 + I^* + \gamma S^*)^2} + \frac{\beta V^*}{K_1 + V^*} + \frac{K_1 \beta S^*}{(K_1 + V^*)^2} < \mu + \frac{\alpha_2 Z^*}{d_2 + \gamma S^*};$$

then  $(|L_S| + |G_S| + G_I + L_V + |G_Z|)_{E^*} < 0$  if

$$\frac{\beta V^*}{K_1 + V^*} + \frac{\alpha_2 \gamma I^* Z^*}{(d_2 + I^* + \gamma S^*)^2} + \frac{\alpha_2 I^*}{d_2 + I^* + \gamma S^*} < \mu + \delta + \frac{\beta S^*}{K_1} + \frac{\alpha_2 Z^*}{d_2 + \gamma S^*};$$

and finally  $(|L_S| + |H_S| + |L_I| + |H_I| + L_V)_{E^*} < 0$  if

$$b\mu + \frac{\beta V^*}{K_1 + V^*} + \frac{\lambda_1 \alpha_1 d_1 Z^*}{(d_1 + S^*)^2} + \frac{\lambda_2 \alpha_2 \{d_2 + \gamma(S^* + I^*)\} Z^*}{(d_2 + I^* + \gamma S^*)^2} < \delta + \frac{\beta S^*}{K_1}.$$

Hence the condition (25).

### 3.5 Hopf-bifurcation analysis

In this section, we show that at the coexistence equilibrium  $E^*$  a Hopf-bifurcation arises, by taking the intensity of avoidance,  $\gamma$ , as bifurcation parameter while keeping the other parameters fixed. More specifically, we have the following result.

**Theorem 4** *The coexistence equilibrium  $E^*$  enters into Hopf-bifurcation as  $\gamma \geq 0$  crosses the critical threshold  $\gamma^*$ , this value being defined as a positive root of the equation  $\psi(\gamma) = 0$ , where  $\psi : (0, \infty) \rightarrow \mathbb{R}$  represents the following continuously differentiable function of  $\gamma$ :*

$$\psi(\gamma) = \sigma_1(\gamma)\sigma_2(\gamma)\sigma_3(\gamma) - \sigma_3^2(\gamma) - \sigma_4(\gamma)\sigma_1^2(\gamma).$$

330 *The Hopf-bifurcation occurs if and only if the condition*

$$\sigma_1^2(\sigma_1\sigma_4' - \sigma_2'\sigma_3) - (\sigma_1\sigma_2 - 2\sigma_3)(\sigma_1\sigma_3' - \sigma_1'\sigma_3) \neq 0, \quad (26)$$

331 *holds and all other eigenvalues have negative real parts.*

332 *Proof* Using the condition  $\psi(\gamma^*) = 0$ , the characteristic equation (23) can be rewritten as

$$\left(\rho^2 + \frac{\sigma_3}{\sigma_1}\right) \left(\rho^2 + \sigma_1\rho + \frac{\sigma_1\sigma_4}{\sigma_3}\right) = 0. \quad (27)$$

333 Let the roots of the above equation be denoted by  $\rho_i$ ,  $i = 1, 2, 3, 4$  and the pair of purely imaginary  
334 roots at  $\gamma = \gamma^*$  be  $\rho_1$  and  $\rho_2$ . We then have

$$\rho_3 + \rho_4 = -\sigma_1, \quad (28)$$

$$\omega_0^2 + \rho_3\rho_4 = \sigma_2, \quad (29)$$

$$\omega_0^2(\rho_3 + \rho_4) = -\sigma_3, \quad (30)$$

$$\omega_0^2\rho_3\rho_4 = \sigma_4, \quad (31)$$

335 where  $\omega_0 = \text{Im}(\rho_1(\gamma^*))$ . By (31) we find  $\omega_0 = \sqrt{\sigma_3\sigma_1^{-1}}$ . Now, if  $\rho_3$  and  $\rho_4$  are complex conjugate  
336 then from (28), it follows that  $2\text{Re}(\rho_3) = -\sigma_1$ ; if they are real roots, recalling that  $\sigma_4 > 0$  by the  
337 Routh-Hurwitz conditions, then by (31) they must have the same sign and from (28) they must be  
338 negative, i.e.  $\rho_3 < 0$  and  $\rho_4 < 0$ . To complete the discussion, it remains to verify the transversality  
339 condition.

340 As  $\psi(\gamma^*)$  is a continuous function of all its roots, there exists an open interval  $I_{\gamma^*} = (\gamma^* - \epsilon, \gamma^* + \epsilon)$ ,  
341 where  $\rho_1$  and  $\rho_2$  are complex conjugate for all  $\gamma \in I_{\gamma^*}$ . Let their general forms in this neighborhood be

$$\rho_1(\gamma) = \chi(\gamma) + i\xi(\gamma), \quad \rho_2(\gamma) = \chi(\gamma) - i\xi(\gamma).$$

342 Substituting  $\rho_j(\gamma) = \chi(\gamma) \pm i\xi(\gamma)$ , into the characteristics equation  $D(\rho) = 0$  and calculating the  
343 derivative, we have

$$L_1(\gamma)\chi'(\gamma) - L_2(\gamma)\xi'(\gamma) + L_3(\gamma) = 0, \quad L_2(\gamma)\chi'(\gamma) + L_1(\gamma)\xi'(\gamma) + L_4(\gamma) = 0,$$

344 where

$$L_1(\gamma) = 4\chi^3 - 12\chi\xi^2 + 3\sigma_1(\chi^2 - \xi^2) + 2\sigma_2\chi + \sigma_3, \quad L_2(\gamma) = 12\chi^2\xi - 4\xi^3 + 6\sigma_1\chi\xi + 2\sigma_2\xi,$$

$$L_3(\gamma) = \sigma_1'\chi^3 - 3\sigma_1'\chi\xi^2 + \sigma_2'(\chi^2 - \xi^2) + \sigma_3'\chi + \sigma_4', \quad L_4(\gamma) = 3\sigma_1'\chi^2\xi - \sigma_1'\xi^3 + 2\sigma_2'\chi\xi + \sigma_3'\xi.$$

345 For  $\gamma = \gamma^*$ , we obtain

$$\begin{aligned} L_1(\gamma^*) &= -2\sigma_3, \quad L_2(\gamma^*) = 2\sqrt{\frac{\sigma_3}{\sigma_1}} \left\{ \sigma_2 - \frac{2\sigma_3}{\sigma_1} \right\}, \\ L_3(\gamma^*) &= \sigma'_4 - \frac{\sigma'_2\sigma_3}{\sigma_1}, \quad L_4(\gamma^*) = \sqrt{\frac{\sigma_3}{\sigma_1}} \left( \sigma'_3 - \frac{\sigma'_1\sigma_3}{\sigma_1} \right). \end{aligned}$$

346 Solving for  $\chi'(\gamma)$  at  $\gamma = \gamma^*$ , we have

$$\begin{aligned} \frac{d}{d\gamma}(Re\rho_j(\gamma))|_{\gamma=\gamma^*} = \chi'(\gamma^*) &= -\frac{L_2(\gamma^*)L_4(\gamma^*) + L_1(\gamma^*)L_3(\gamma^*)}{L_1^2(\gamma^*) + L_2^2(\gamma^*)} \\ &= \frac{\sigma_1^2(\sigma_1\sigma'_4 - \sigma'_2\sigma_3) - (\sigma_1\sigma_2 - 2\sigma_3)(\sigma_1\sigma'_3 - \sigma'_1\sigma_3)}{2\sigma_1^3\sigma_3 + 2(\sigma_1\sigma_2 - 2\sigma_3)^2} \neq 0 \end{aligned}$$

347 if (26) is satisfied. Thus the transversality condition holds and hence the claim.

348 To better understand the nature of the instability, we determine the initial period and the amplitude  
349 of the oscillatory solutions. From (28)–(31), solving (30) for  $\omega^2$  and substituting from (28) we get  
350  $\omega^2 = \sigma_3\sigma_1^{-1}$ . Obtaining  $\sigma_4$  from (31) and combining with the previous result, we find  $\sigma_4 = \sigma_3\rho_3\rho_4\sigma_1^{-1}$ .  
351 The quantity  $\rho_3\rho_4$  is obtained then from (29), and thus leads to the expression  $\sigma_4 = \sigma_3(\sigma_1\sigma_2 - \sigma_3)\sigma_1^{-2}$ .  
352 Then relaxing it to  $\sigma_4(\psi) = \psi\sigma_4$  and substituting into equation (23), if  $\rho$  depends continuously on  $\psi$ ,  
353 we can rewrite equation (23) as

$$\rho^4 + \sigma_1\rho^3 + \sigma_2\rho^2 + \sigma_3\rho + \frac{\psi\sigma_3(\sigma_1\sigma_2 - \sigma_3)}{\sigma_1^2} = 0. \quad (32)$$

354 At  $\psi = \psi^* = 1$ , because  $\sigma_1^2\sigma_4 = \sigma_3(\sigma_1\sigma_2 - \sigma_3)$ , equation (23) factorizes into the form (27) which  
355 has a pair of purely imaginary roots,  $\rho(\psi^*) = \pm i\sqrt{\sigma_3\sigma_1^{-1}}$  while the other two roots are either negative  
356 or have negative real parts. This substantiates the claim that the Hopf-bifurcation is present.

357 Further, if  $\psi \in (0, 1)$ , then  $\sigma_1^2\sigma_4 - \sigma_3(\sigma_1\sigma_2 - \sigma_3)$  is positive, which assures stability, and conversely  
358 for  $\psi > 1$ , we obtain instability.

359 Observe now that  $\rho$  is a function of  $\psi$ . We differentiate equation (32) with respect to  $\psi$ , denoting  
360 this operation by a prime. By setting  $\psi = \psi^* + \epsilon^2\xi$ , where  $|\epsilon| \ll 1$  and  $\xi = \pm 1$ , then  $\rho(\psi) = \rho(\psi^* + \epsilon^2\xi)$   
361 so that expanding in Taylor series of  $\rho$  around  $\psi^*$  up to the first order, we find

$$\rho(\psi) = \rho(\psi^*) + \rho'(\psi^*)\epsilon^2\xi + O(\epsilon^4). \quad (33)$$

362 Replacing  $\rho(\psi^*)$  by  $i \pm \sqrt{\frac{\sigma_3}{\sigma_1}}$  in the derivative and conjugating the expression for the derivative we get  
363 equation

$$\rho'(\psi^*) \equiv \frac{\sigma_1\sigma_3(\sigma_1\sigma_2 - \sigma_3)}{2[\sigma_1^3\sigma_3 + (\sigma_1\sigma_2 - 2\sigma_3)^2]} \pm i\sqrt{\frac{\sigma_3}{\sigma_1}} \frac{(\sigma_1\sigma_2 - \sigma_3)(\sigma_1\sigma_2 - 2\sigma_3)}{2[\sigma_1^3\sigma_3 + (\sigma_1\sigma_2 - 2\sigma_3)^2]}. \quad (34)$$

Using the fact that

$$\Re(\rho(\psi^*)) = 0, \quad \Re(\rho'(\psi^*)) = \frac{\sigma_1\sigma_3(\sigma_1\sigma_2 - \sigma_3)}{2[\sigma_1^3\sigma_3 + (\sigma_1\sigma_2 - 2\sigma_3)^2]} > 0$$

and substituting  $\rho(\psi^*)$  and  $\rho'(\psi^*)$  into equation (33), we obtain the approximation

$$\begin{aligned} \rho(\psi) &= \rho(\psi^*) + \rho'(\psi^*)\epsilon^2\xi \\ &= \frac{\sigma_1\sigma_3(\sigma_1\sigma_2 - \sigma_3)\epsilon^2\xi}{2[\sigma_1^3\sigma_3 + (\sigma_1\sigma_2 - 2\sigma_3)^2]} \pm i\sqrt{\frac{\sigma_3}{\sigma_1}} \left( 1 + \frac{(\sigma_1\sigma_2 - \sigma_3)(\sigma_1\sigma_2 - 2\sigma_3)\epsilon^2\xi}{2[\sigma_1^3\sigma_3 + (\sigma_1\sigma_2 - 2\sigma_3)^2]} \right) + O(\epsilon^4). \end{aligned} \quad (35)$$

Setting  $\epsilon = \sqrt{|\psi - \psi^*|} \times |\xi|^{-1}$ , the initial period and amplitude of the oscillations associated with the loss of stability when  $\psi > \psi^*$  respectively are

$$\frac{2\pi}{\sqrt{\frac{\sigma_3}{\sigma_1} \left( 1 + \frac{(\sigma_1\sigma_2 - \sigma_3)(\sigma_1\sigma_2 - 2\sigma_3)\epsilon^2\xi}{2[\sigma_1^3\sigma_3 + (\sigma_1\sigma_2 - 2\sigma_3)^2]} \right)}}, \quad \exp\left(\frac{\sigma_1\sigma_3(\sigma_1\sigma_2 - \sigma_3)\epsilon^2\xi}{2[\sigma_1^3\sigma_3 + (\sigma_1\sigma_2 - 2\sigma_3)^2]}\right).$$

#### 4 Simulations of the ecosystem behavior

Here, we report the simulations to investigate the behavior of system (1), performed using the Matlab variable step Runge-Kutta solver ode45. The set of parameter values are chosen within the range prescribed in various previous literature sources [14, 15, 52], and are given in Table 1.

##### 4.1 Sensitivity analysis

To assess the sensitivity of the solutions to variations in the model parameters partial rank correlation coefficient (PRCC), a global sensitivity analysis technique that is proven to be the most reliable and efficient among the sampling-based methods, is utilized. The PRCC determines the effect of changes in a specific parameter, by discounting linearly the influences over the other parameters, on the reference model output [60]. In order to obtain the PRCC values, Latin Hypercube Sampling (LHS) is chosen for the input parameters by performing a stratified sampling without replacement. In the current study, a uniform distribution is assigned to each model parameter and sampling is performed independently. The range for each parameter is initially set to  $\pm 25\%$  of the nominal values given in Table 1. A total of 200 simulations are considered, wherein a set of parameter values are selected from the uniform distribution.

Note that the PRCC values lie between  $-1$  and  $1$ . Positive (negative) values indicate a positive (negative) correlation of the parameter with the model output. A positive (negative) correlation implies that a positive (negative) change in the parameter will increase (decrease) the model output. The larger

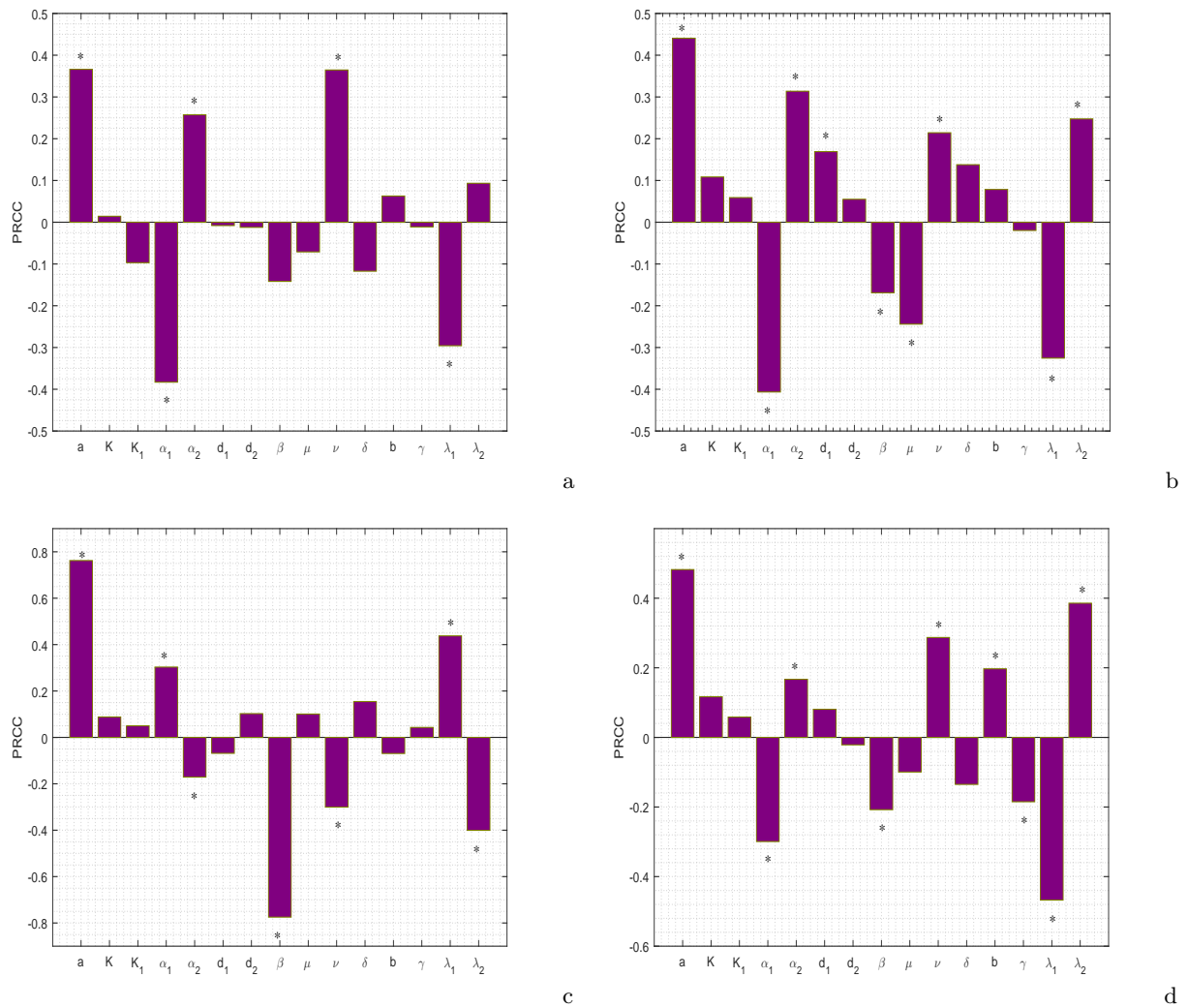


**Fig. 2** Effect of uncertainty of the model (1) on (a)  $S$ , (b)  $I$ , (c)  $Z$  and (d)  $V$ . Significant parameters are marked by \* for  $p < 0.01$ . Baseline values of the parameter are the same as in Table 1.

383 the absolute value of the PRCC, the greater the correlation of the parameter with the output. The  
 384 bar diagram of the PRCC values of susceptible phytoplankton, infected phytoplankton, zooplankton  
 385 and free viruses against the parameters is depicted in Fig. 2. It therefore emerges that susceptible  
 386 phytoplankton is significantly correlated with the model parameters  $a$ ,  $\alpha_1$ ,  $\alpha_2$ ,  $\nu$  and  $\lambda_1$ , while for the  
 387 infected phytoplankton, the most influential parameters appear to be  $a$ ,  $\alpha_1$ ,  $\alpha_2$ ,  $d_1$ ,  $\beta$ ,  $\mu$ ,  $\nu$ ,  $\lambda_1$  and  
 388  $\lambda_2$ . Further, the parameters  $a$ ,  $\alpha_1$ ,  $\alpha_2$ ,  $\beta$ ,  $\nu$ ,  $\lambda_1$  and  $\lambda_2$  instead significantly affect zooplankton. Finally,  
 389 free viruses are mostly dependent on the parameters  $a$ ,  $\alpha_1$ ,  $\alpha_2$ ,  $\beta$ ,  $\nu$ ,  $b$ ,  $\gamma$ ,  $\lambda_1$  and  $\lambda_2$ .

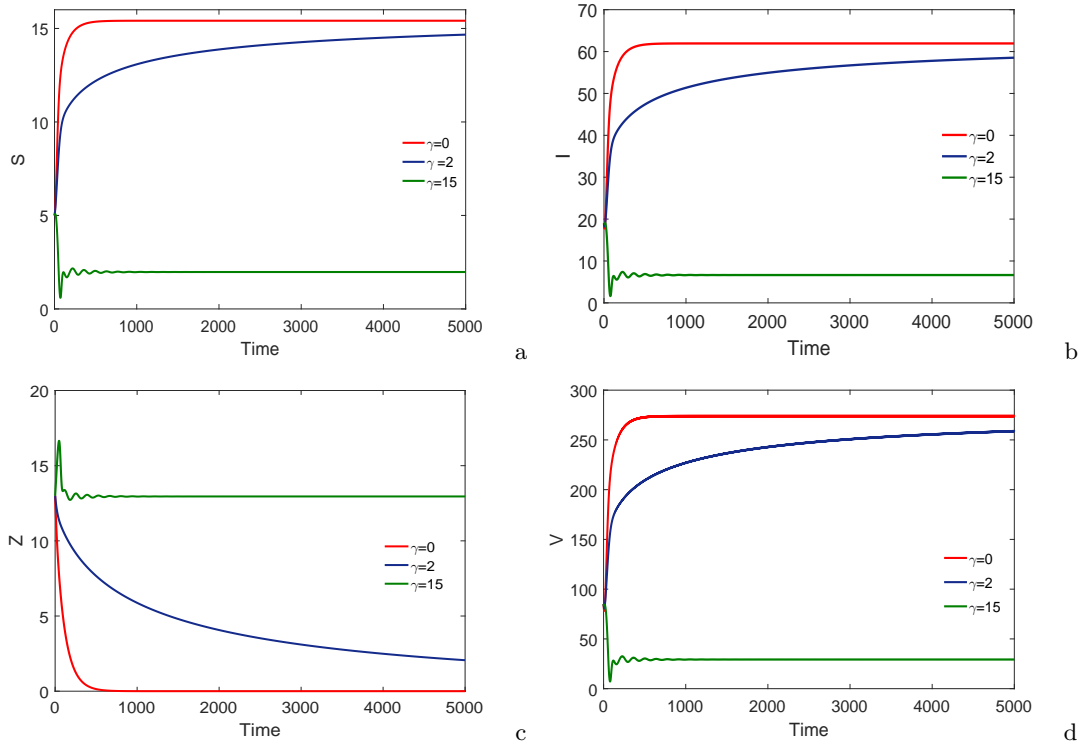


**Fig. 3** Variations of susceptible phytoplankton ( $S$ ), infected phytoplankton ( $I$ ), zooplankton ( $Z$ ) and free-viruses ( $V$ ) with respect to time for different values of  $\gamma$ . Rest of the parameter values are the same as in Table 1.

390 4.2 Effect on the ecosystem behavior on variations of the model parameters

391 We see the impact of avoidance parameter,  $\gamma$ , on the equilibrium values of each variables of the system  
 392 (1), Fig. 3. We see that the abundances of susceptible phytoplankton, infected phytoplankton and  
 393 free-viruses are at higher values when the zooplankton do not discriminate between susceptible and  
 394 infected phytoplankton. For the non-zero values of  $\gamma$ , the zooplankton discriminate between susceptible  
 395 and infected phytoplankton. As the value of  $\gamma$  increases, both type of phytoplankton and free-viruses  
 396 decrease in the system. For very large values of  $\gamma$ , the phytoplankton and free-viruses settle to very low  
 397 equilibrium values. Interestingly, the zooplankton population become zero for large time in the case  
 398 when they do not discriminate between susceptible and infected phytoplankton, as the ingestion of  
 399 infected phytoplankton increases the death rate of zooplankton. As the values of avoidance parameter  
 400 increases, the zooplankton move away from the infected phytoplankton, and ingest them at a very low  
 401 rate. This results in lesser death of zooplankton, and hence their abundance increase with increase in  
 402 the values of  $\gamma$ . For very large values of  $\gamma$ , the zooplankton population attains high equilibrium values.



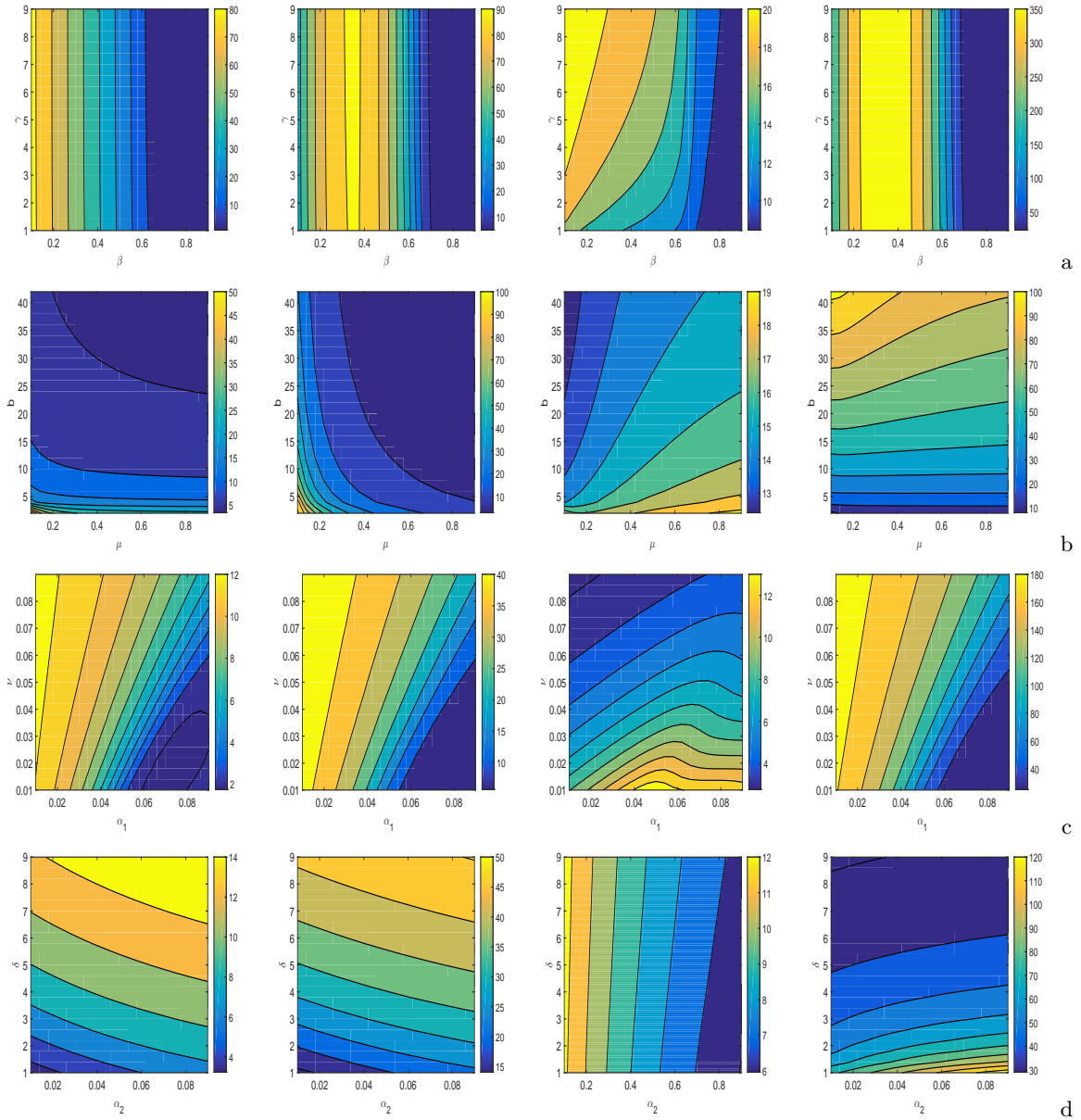


**Fig. 4** Contour lines representing the equilibrium values of susceptible phytoplankton (first column), infected phytoplankton (second column), zooplankton (third column) and free viruses (fourth column) as functions of (a)  $\beta$  and  $\gamma$ , (b)  $\mu$  and  $b$ , (c)  $\alpha_1$  and  $\nu$ , and (d)  $\alpha_2$  and  $\delta$ . Rest of the parameter values are the same as in Table 1.

403 Next, we see how equilibrium abundances of ecosystem populations change by varying some of the  
 404 input parameters, namely  $\beta$ ,  $\gamma$ ,  $\mu$ ,  $b$ ,  $\alpha_1$ ,  $\alpha_2$ ,  $\nu$  and  $\delta$ . By varying two parameters at a time in biolog-  
 405 ically meaningful regions, we plot contour lines for the surfaces representing the system populations,  
 406 Fig. 4. It is apparent from Fig. 4(a) that the concentration of zooplankton increases with increase in  
 407 the intensity of avoidance  $\gamma$ , but for the remaining populations this parameter is instead much less

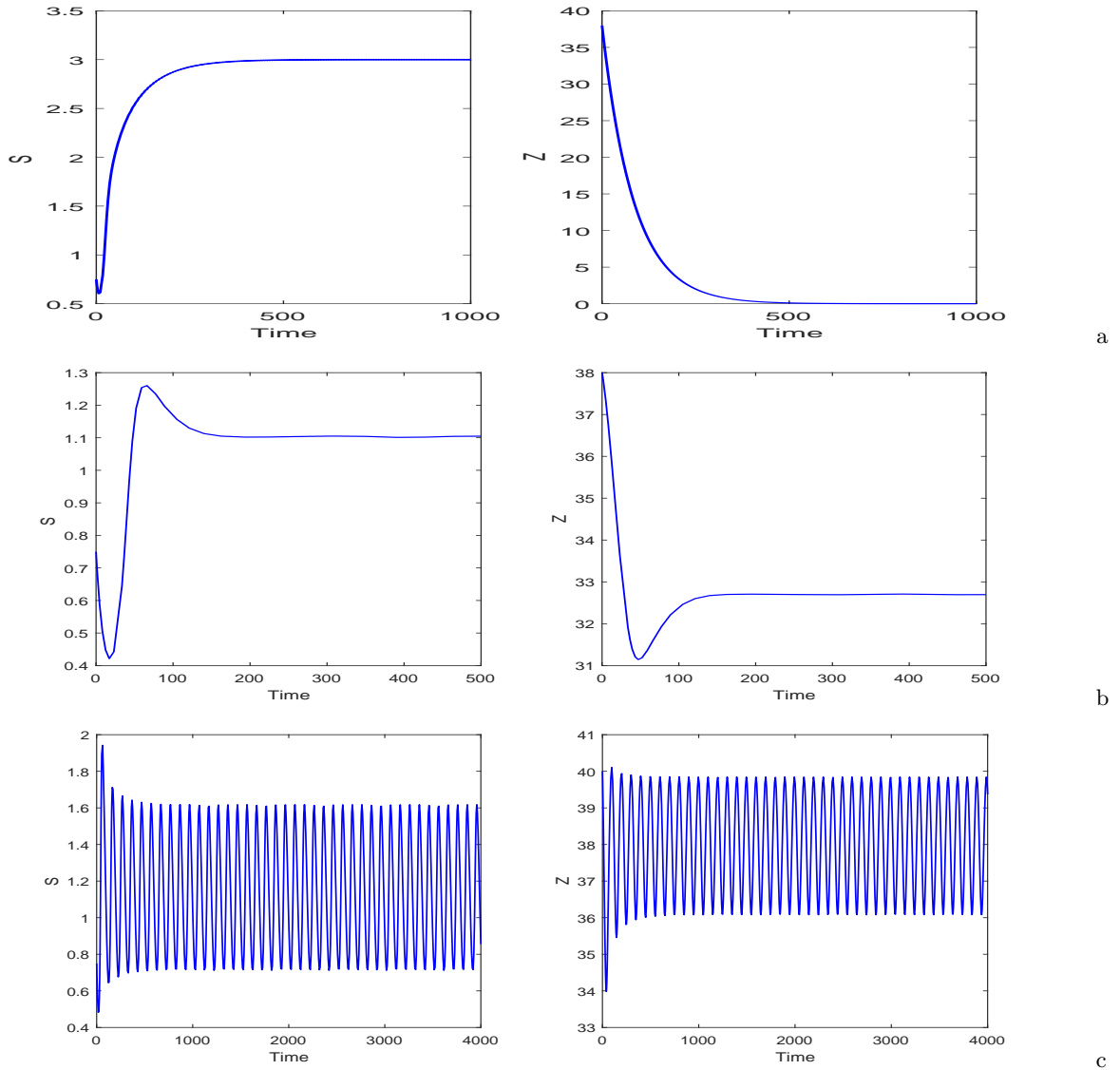


**Fig. 5** For virus-free environment ( $I = 0$  and  $V = 0$ ) i.e., subsystem (3): (a) zooplankton-free equilibrium is achieved at  $K = 3$  and  $\lambda_1 = 0.01$ . System (3) shows (b) stable coexistence at  $K = 3$  and  $\lambda_1 = 0.75$ , and (c) limit cycle oscillations around the coexistence equilibrium at  $K = 4.3$  and  $\lambda_1 = 0.75$ . Rest of the parameters are at the same values as in Table 1.

408 influential. On increasing the force of infection  $\beta$ , the concentrations of susceptible phytoplankton and  
 409 zooplankton decrease while those of infected phytoplankton and free viruses initially increase and then  
 410 decrease. Fig. 4(b) shows that with an increase in the death rate of infected phytoplankton  $\mu$ , the  
 411 concentration of infected phytoplankton decreases but that of zooplankton increases. On increasing  
 412 the virus-replication factor  $b$ , the susceptible phytoplankton and zooplankton populations decrease  
 413 but the free viruses increase significantly. Looking at Fig. 4(c), we may note that the concentration of

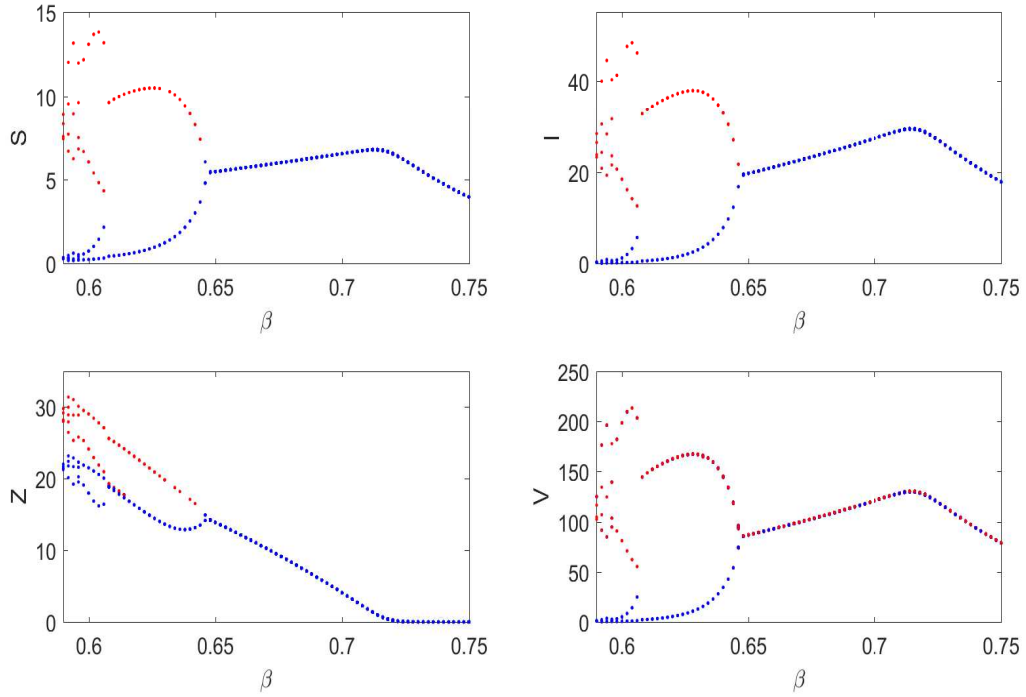


**Fig. 6** Bifurcation diagram of the system (1) with respect to force of infection  $\beta$ . Here, the maximum and minimum values of the oscillations are plotted in red and blue colors, respectively. Rest of the parameter values are the same as in Table 1.

414 susceptible phytoplankton for low values of  $\alpha_1$  decreases by increasing this parameter. The same situ-  
 415 ations occurs for the infected phytoplankton and the free viruses. However, zooplankton benefits by an  
 416 increase in the values of  $\alpha_1$ . On increasing the zooplankton mortality rate, susceptible phytoplankton,  
 417 infected phytoplankton and free viruses all increase, but the zooplankton population attains very low  
 418 equilibrium values. From Fig. 4(d) increasing the values of  $\alpha_2$ , leads to higher values of susceptible  
 419 phytoplankton, infected phytoplankton and viruses, while zooplankton decrease. On increasing the  
 420 free viruses mortality rate  $\delta$ , susceptible and infected phytoplankton increase, the latter slightly, while  
 421 free viruses decrease. Zooplankton essentially are not affected by  $\delta$ . Looking at the combined effect of  
 422  $\alpha_2$  and  $\delta$ , we observe that along the main diagonal the susceptible phytoplankton increase while free  
 423 viruses decrease.

#### 424 4.3 Existence of Hopf-bifurcation and Transcritical bifurcation

425 First, we investigate the dynamics of the system (1) in the absence of free viruses and infected phyto-  
 426 plankton. For system (3), note that the zooplankton-free equilibrium  $e_1$  is related to the coexistence

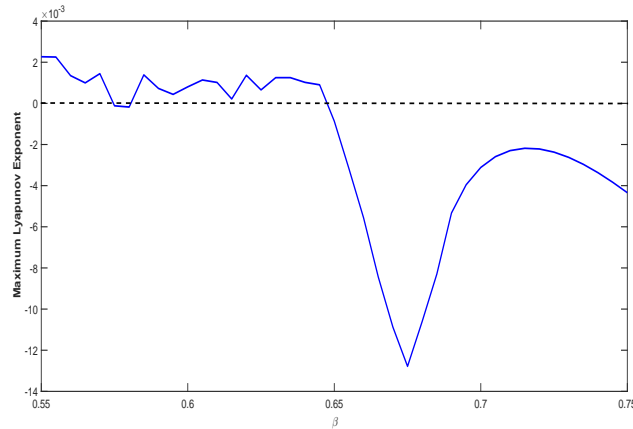


**Fig. 7** Variation of the maximum Lyapunov exponent with respect to  $\beta$  for the model (1), where other parameter values are the same as in Table 1. The maximum Lyapunov exponent becomes negative from positive values, which confirms that the system (1) becomes stable from chaotic dynamics for increase in the values of parameter  $\beta$ .

427 equilibrium  $e_*$  via a transcritical bifurcation taking  $\lambda_1$  as a bifurcation parameter. For low values of  
 428  $\lambda_1$  ( $\lambda_1 = 0.01$ ,  $K = 3$ ), the zooplankton-free equilibrium  $e_1$  is stable, Fig. 5(a), while the zooplankton-  
 429 free equilibrium  $e_1$  loses its stability and the coexistence equilibrium  $e_*$  emanates from the former  
 430 on increasing the values of  $\lambda_1$  past a critical threshold, specifically for  $\lambda_1 = 0.75$ ,  $K = 3$ , Fig. 5(b).  
 431 Further, observe that on increasing the values of  $K$ , specifically  $\lambda_1 = 0.75$ ,  $K = 4.3$ , the coexistence  
 432 equilibrium  $e_*$  loses its stability and persistent oscillations occur, Fig. 5(c), that are found also by a  
 433 further increase in the values of  $K$ . For the model (1), stability of the disease-free equilibrium  $E_2$  can  
 434 be obtained with  $K = 3.4$ ,  $\beta = 0.12$  and  $K_1 = 1.6$ , while the remaining parameter values appear in  
 435 Table 1. Now, we see how dynamics of the system (1) changes on varying the force of infection  $\beta$ ,  
 436 virus replication factor  $b$ , intensity of avoidance  $\gamma$  and carrying capacity  $K$ , while keeping the values of  
 437 remaining parameters as in Table 1. We vary the parameter  $\beta$  in the interval  $[0.59, 0.75]$  and note the  
 438 different behaviors of system (1), Fig. 6. At  $\beta = 0.59$ , we observe that the system (1) shows chaotic  
 439 dynamics; at  $\beta = 0.6$  the system exhibits period halving oscillations; at  $\beta = 0.62$ , the system shows  
 440 limit cycle oscillation; at  $\beta = 0.65$ , the system shows stable focus. We find that for large values of  $\beta$ ,  
 441 namely  $\beta = 0.74$ , the system settles down to the zooplankton-free steady state. Thus, there exists a  
 442 transcritical bifurcation between equilibria  $E_3$  and  $E^*$  where  $\beta$  represents the bifurcation parameter;  
 443 the former arises while the latter loses its stability as  $\beta$  crosses its critical value from below. The most  
 444 important mathematical attribute of chaos is the absence of any stable equilibrium point or any stable  
 445 limit cycle in system dynamics, for which the patterns never repeat themselves. We also report the

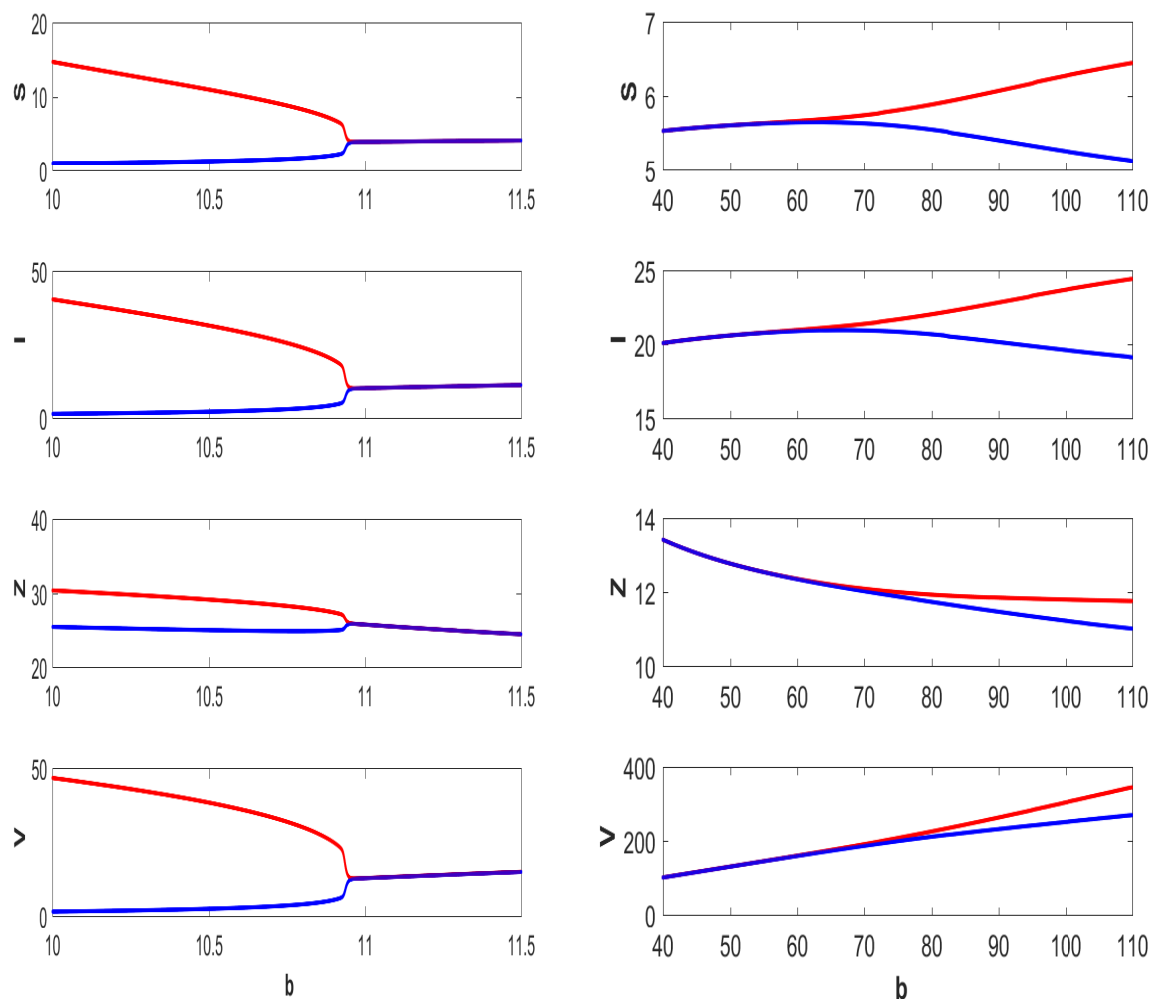


**Fig. 8** Bifurcation diagram of the system (1) with respect to virus replication factor  $b$ . The two columns correspond to two very different ranges for this parameter value. Here, the maximum and minimum values of the oscillations are plotted in red and blue colors, respectively. Rest of the parameter values are the same as in Table 1.

446 maximum Lyapunov exponent with respect to  $\beta$  in Fig. 7, its positive values indicating the chaotic  
 447 regime of the system.

448 Further, to visualize the effect of the virus replication factor on the system dynamics, we draw  
 449 the bifurcation diagram by taking  $b$  as a bifurcation parameter, Fig. 8. Increasing the values of  $b$ , two  
 450 critical values of  $b$  are found,  $b_H^1 = 10.96$  and  $b_H^2 = 65.15$ , so that for  $b < b_H^1$ , limit cycle oscillations  
 451 are observed, for  $b_H^1 < b < b_H^2$ , the system stabilizes, while for  $b > b_H^2$  again persistent oscillations

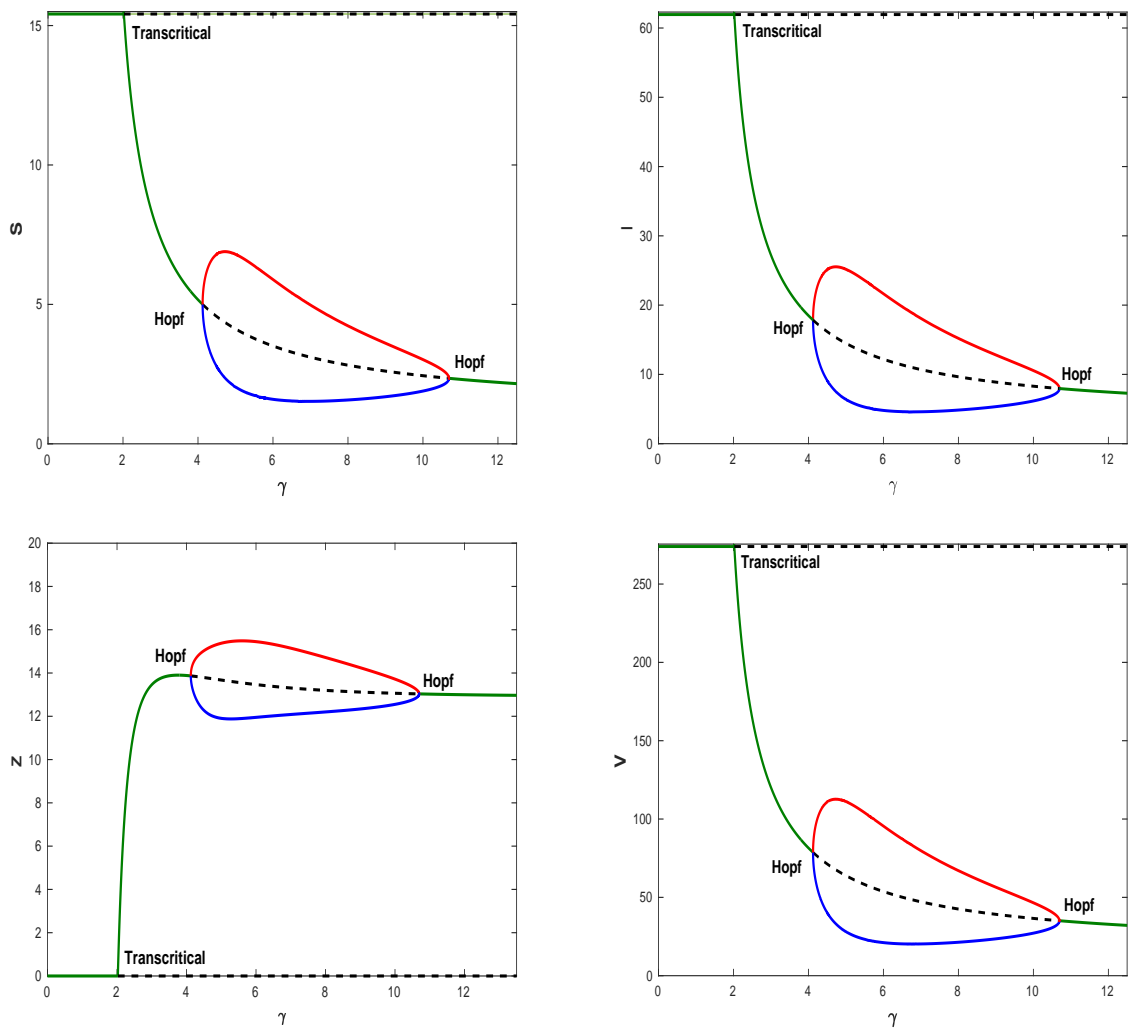


**Fig. 9** Bifurcation diagram of the system (1) with respect to avoidance intensity,  $\gamma$ . Here, the maximum and minimum values of the oscillations are plotted in red and blue colors, respectively. Rest of the parameter values are the same as in Table 1.

452 appear. Furthermore, a bifurcation diagram in terms of the avoidance intensity  $\gamma$  is shown in Fig. 9. For  
 453 low values of  $\gamma$ , the zooplankton-free equilibrium is stable, while on increasing it at the critical value  
 454  $\gamma_T = 1.99$  the coexistence equilibrium emanates from the former. Further, there exist two critical values  
 455 of  $\gamma$ , namely  $\gamma_H^1 = 4.05$  and  $\gamma_H^2 = 10.95$ , such that at  $\gamma = \gamma_H^1$ , the system undergoes a supercritical  
 456 Hopf-bifurcation and produces oscillations. Keeping on increasing the value of  $\gamma$ , the system undergoes  
 457 a subcritical Hopf-bifurcation at  $\gamma = \gamma_H^2$  after which it stabilizes again. Therefore, this ecosystem may  
 458 show multiple stability switching depending on the values of virus replication factor and avoidance  
 459 intensity. Note that in Fig. 9 we have chosen  $\beta = 0.65$ , which lies in the stable region of Fig. 6. Now,

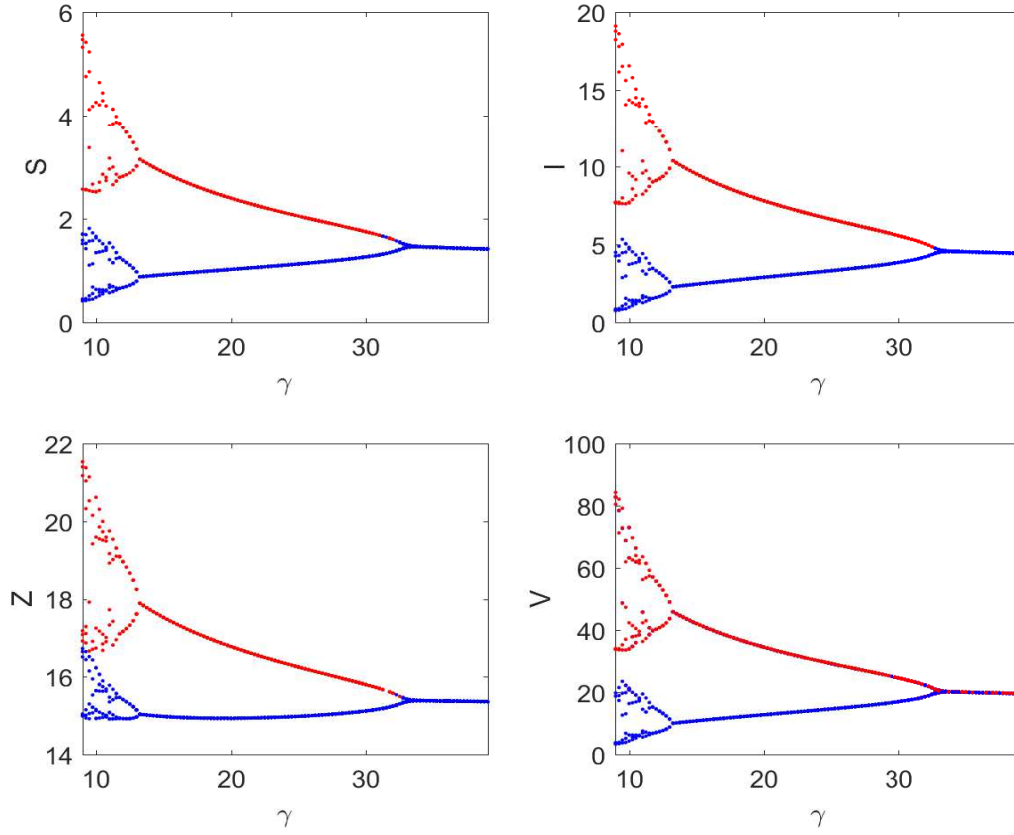


**Fig. 10** Chaotic behavior of the system (1) with respect to intensity of avoidance ( $\gamma$ ). Here, the maximum and minimum values of the oscillations are plotted in red and blue colors, respectively. Rest of the parameter values are the same as in Table 1 except  $\beta = 0.62$ .

460 we set  $\beta = 0.62$ , in the Hopf-region of Fig. 6, while keeping all the other parameters as in Table 1.  
 461 We obtain that varying the avoidance parameter  $\gamma$  in the interval  $[9, 39]$ , Fig. 10, stable coexistence is  
 462 achieved via a chaotic regime through period halving oscillations. The combined effect of the avoidance  
 463 parameter  $\gamma$  and of the force of infection  $\beta$  are seen in Fig. 11, that portrays the different stability  
 464 regions of the system (1). Here, blue, red, orange and green colors respectively represent the chaotic,  
 465 period halving, limit cycle oscillation and stability domains. For higher values of the avoidance intensity,  
 466 the ecosystem may show different stability behavior on increasing the force of infection. It goes possibly  
 467 from chaos to period halving oscillations to limit cycle oscillations and finally to a stable focus. For  
 468 intermediate values of  $\beta$ , the ecosystem experiences limit cycle oscillation to period doubling oscillation  
 469 to chaotic behavior by increasing  $\gamma$ . Further simulations that are not reported indicate that for higher  
 470 values of  $\gamma$ , chaos can be controlled and the system attains a stable focus. The stable equilibrium enters

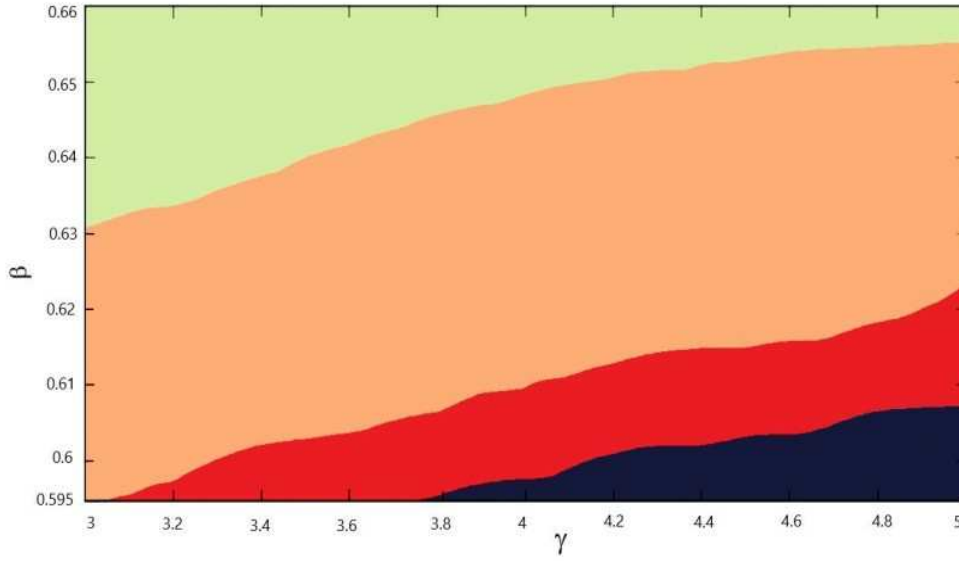


**Fig. 11** Two-parameter bifurcation diagram as a function of  $\gamma$  and  $\beta$ . Regions in blue, red, orange and green colors represent chaotic, period halving, limit cycle and stable domains, respectively. Rest of the parameter values are the same as in Table 1.

471 into a chaotic regime through period doubling high-amplitude oscillations by increasing the values of  
 472  $K$ , i.e., increasing the nutrient supply, Fig. 12. This result is in line with the *paradox of enrichment*  
 473 [61].

474 Next, we observe how the dynamics of the system changes if the susceptible phytoplankton feels  
 475 the intraspecific pressure due to infected phytoplankton [39]. In such case, system (1) is reformulated  
 476 as,

$$\begin{aligned}
 \frac{dS}{dt} &= aS \left( 1 - \frac{S+I}{K} \right) - \frac{\alpha_1 SZ}{d_1 + S} - \frac{\beta SV}{K_1 + V}, \\
 \frac{dI}{dt} &= \frac{\beta SV}{K_1 + V} - \frac{\alpha_2 IZ}{d_2 + I + \gamma S} - \mu I, \\
 \frac{dZ}{dt} &= \frac{\lambda_1 \alpha_1 SZ}{d_1 + S} - \frac{\lambda_2 \alpha_2 IZ}{d_2 + I + \gamma S} - \nu Z, \\
 \frac{dV}{dt} &= b\mu I - \frac{\beta SV}{K_1 + V} - \delta V.
 \end{aligned} \tag{36}$$

477 The dynamics of (36) is investigated only by numerical simulations and compared with the findings of  
 478 system (1). For low values of  $\beta$ , system (36) shows limit cycle oscillations but the oscillations vanish  
 479 for increasing values of  $\beta$ , and for very high value of  $\beta$ , the zooplankton disappears from the system,  
 480 Fig. 13(a). For low values of  $\beta$ , system (1) exhibits instead chaotic dynamics. Further, for low values  
 481 of  $b$ , system (36) shows chaotic dynamics, but on increasing the values of  $b$  it switches to a stable focus



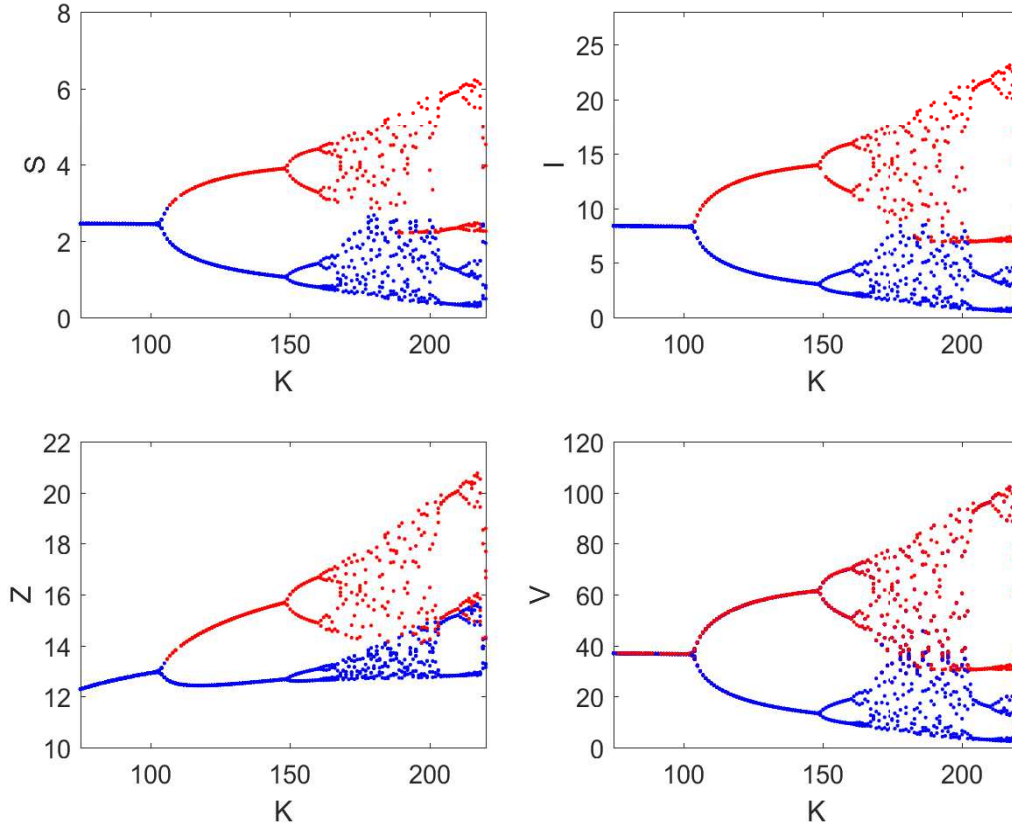


**Fig. 12** Bifurcation diagram of the system (1) with respect to carrying capacity of the system ( $K$ ). Here, the maximum and minimum values of the oscillations are plotted in red and blue colors, respectively. Rest of the parameter values are the same as in Table 1 except  $\gamma = 10$ .

482 through period halving bifurcation, Fig. 13(b). Moreover, for very high value of the parameter  $b$ , the  
 483 zooplankton population does not survive in the system, Fig. 13(c). Recall that for very low and very  
 484 high values of  $b$ , the system (1) shows limit cycle oscillations, and stable dynamics for moderate values  
 485 of  $b$ . For low values of avoidance parameter,  $\gamma$ , system (36) shows extinction of zooplankton, and stable  
 486 coexistence of all the populations after a threshold value of  $\gamma$ . Previously, we observed that the system  
 487 (1) showed extinction of zooplankton for low values of  $\gamma$ , but on increasing the values of  $\gamma$ , the system  
 488 experienced stability switches from stable to unstable to stable dynamics. We note that for low values  
 489 of  $K$ , the zooplankton population becomes extinct from the system (this behavior is not observed for  
 490 system (1)) but the coexistence equilibrium appears on increasing the values of  $K$ , see Fig. 13(e), and  
 491 the system becomes chaotic for very large values of  $K$ , see Fig. 13(f).

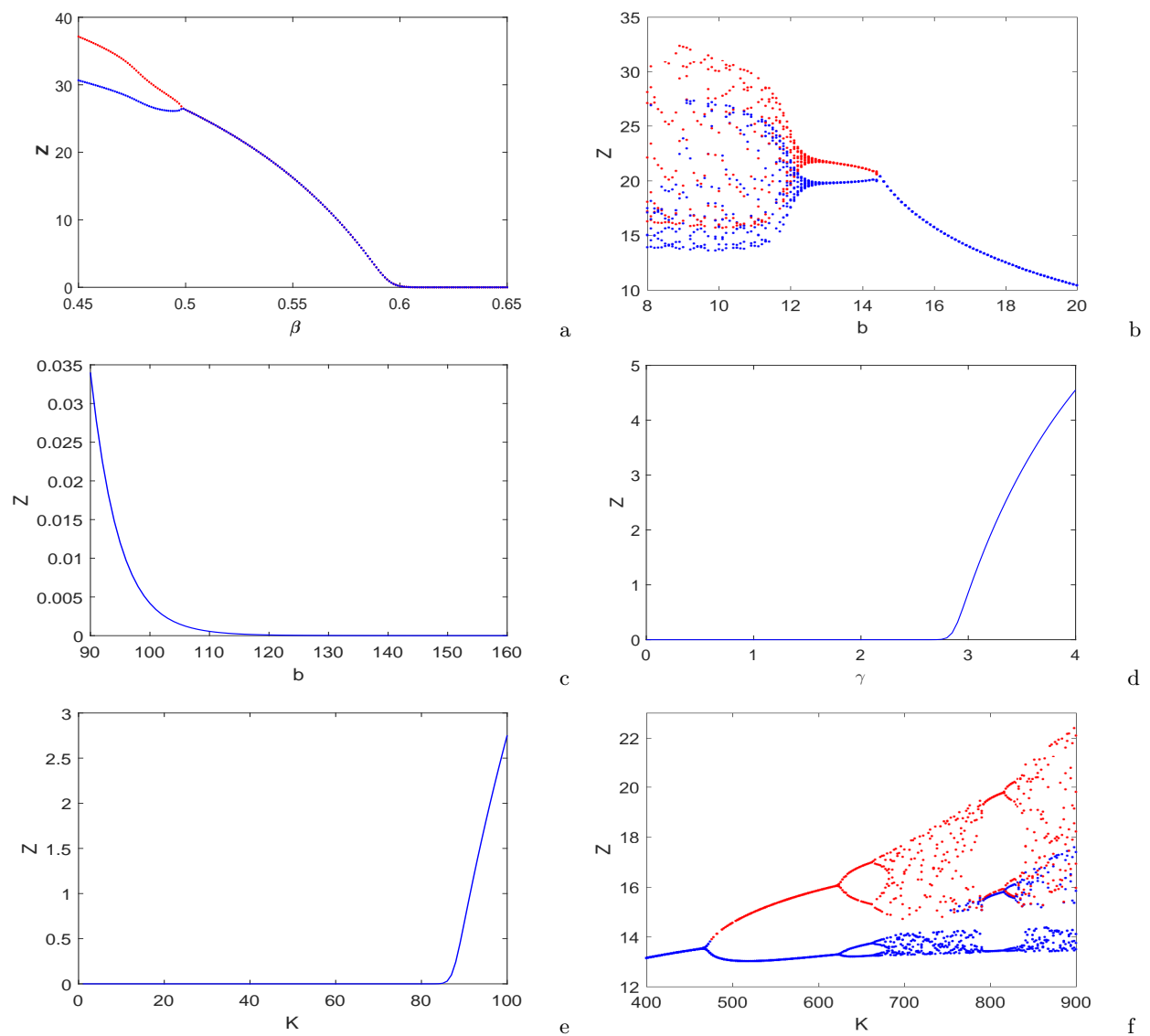


**Fig. 13** System (36) shows (a) limit cycle oscillation for low values of  $\beta$ , (b) chaotic dynamics for low values of  $b$ , (c) extinction of zooplankton for very high value of  $b$ , (d) extinction of zooplankton for low values of  $\gamma$  but stable dynamics after a threshold value of  $\gamma$ , (e) extinction of zooplankton for low values of  $K$ , and (f) chaotic dynamics for very large values of  $K$ . Here, the maximum and minimum values of the oscillations are plotted in red and blue colors, respectively. Parameters are at the same value as in Table 1 except  $\lambda_2 = 0.42$ .

## 492 5 Conclusion and discussion

493 The interest in ecological studies of prey avoidance by a predator ranges from the details of individual  
 494 feeding behavior to the implications for predator-prey dynamics. Some predators have the ability to  
 495 discriminate between different types of prey and show avoidance to some specific prey population  
 496 based on several known and unknown criteria [62]. In this paper, a mathematical model for the study

of the avoidance behavior of zooplankton on infected phytoplankton is proposed and its essential dynamical features are analyzed. The dynamics of free viruses is explicitly considered in the model. The partial rank correlation coefficient (PRCC) technique is performed to assess the sensitivity of the ecosystem with respect to the model parameters. The main parameters influencing the system behavior appear to be  $a$ ,  $K$ ,  $K_1$ ,  $\alpha_2$ ,  $d_1$ ,  $d_2$ ,  $\nu$ ,  $\delta$ ,  $b$  and  $\lambda_2$ . They present positive correlations with the infected phytoplankton. Similarly, the parameters  $\alpha_1$ ,  $d_2$ ,  $\beta$ ,  $\mu$ ,  $\delta$ ,  $\gamma$  and  $\lambda_1$  possess negative correlations with free viruses.

To identify the role of different parameters for the coexistence of all the populations, we use contour plots to represent the populations equilibrium values in terms of some important parameters:  $\beta$ ,  $\gamma$ ,  $\mu$ ,  $b$ ,  $\lambda_1$ ,  $\lambda_2$ ,  $\alpha_1$ ,  $\alpha_2$ ,  $\nu$  and  $\delta$ . From these plots, the force of infection  $\beta$ , the virus replication factor  $b$  and the decay rate of free viruses  $\delta$  appear to be important quantities to control the infection. To reduce disease prevalence in the phytoplankton,  $\beta$  and  $b$  should be reduced while  $\delta$  should be fostered. On the other hand, the avoidance intensity  $\gamma$  fosters species coexistence. In the presence of viral infection, high intensity of zooplankton avoidance triggers the system chaotic behavior from a stable focus, due to nutrient enrichment. There is a minimum strength of the force of infection above which the infection becomes endemic in the system. Interestingly, increasing the infection rate the system switches from chaotic oscillations to a stable endemic equilibrium. Hence, the force of infection can control the chaotic behavior in this eco-epidemiological system. Further increasing the infection rate, the grazer zooplankton becomes extinct past a critical value of the force of infection. Increasing the virus replication factor values, the system stabilizes from persistent oscillations. If the virus replication factor exceeds a threshold value, the system becomes unstable again. Thus, the system shows multiple stability switching as a function of  $b$ , which therefore may play a crucial role in the system dynamics. A similar behavior for multiple stability switching is observed also in terms of the avoidance intensity, for which the system goes from a stable state to persistent oscillations via a supercritical Hopf bifurcation. Later on via another subcritical Hopf bifurcation, it stabilizes again. Our study suggests that the zooplankton's chance of extinction increases for lower values of the avoidance intensity. Interestingly, the avoidance parameter  $\gamma$  possesses a stabilizing role for the aquatic system by terminating the chaotic nature of the system. Thus, the avoidance parameter  $\gamma$  may be treated as a control parameter for the aquatic balance of the food web, indicating that the zooplankton avoidance of infected phytoplankton may significantly affect the ultimate ecosystem behavior.

527 Finally, we compare the dynamics of system (1) i.e., when infected phytoplankton do not compete  
528 for resources with the susceptible, with the system (36) i.e., when infected phytoplankton share re-  
529 sources with the susceptible ones. In the latter case, the system exhibits limit cycle oscillations (chaotic  
530 dynamics) for low values of force of infection (virus replication factor) while in the former case, the  
531 system shows chaotic dynamics (limit cycle oscillations) for low ranges of these two parameters. More-  
532 over, in the second case, the system becomes zooplankton-free for higher values of the virus replication  
533 factor. The limit cycle oscillations also disappear for the second case on increasing the avoidance pa-  
534 rameter, and interestingly the second model shows extinction of zooplankton for low values of the  
535 system carrying capacity.

536 The size of an organism affects virtually all aspects of its physiology and ecology [63]. The zooplank-  
537 ton body size gradually decreases during equilibrium condition in comparison to chaos [50]. Jørgensen  
538 et al. [64] showed that size combinations between phytoplankton and zooplankton are very crucial  
539 for the system's self-organization. The system cannot adapt to the gradual decrease of zooplankton  
540 size and as a result it moves from an equilibrium state to a chaotic condition. It is beneficial for low  
541 zooplankton populations to grow fast. If the fast growth continues the phytoplankton will be rapidly  
542 exhausted and in turn the zooplankton population will plunge, with the consequence that the system  
543 is led into violent oscillations and will ultimately attain chaos. This behavior however is not prevalent  
544 in many ecosystems, because they are self-organizing and self-adapting [65]. They tune themselves to a  
545 critical state [66] and show a high extent of self-organization based upon a hierarchy of feedback mech-  
546 anisms. Among the many ways for which ecosystems can be self-adjusted, we have proposed and shown  
547 here that avoidance of virally infected phytoplankton by zooplankton, which reduces the zooplankton  
548 grazing, could be one of them and would help the system to recover from chaotic situation. These  
549 observations indicate that the avoidance of infected phytoplankton by zooplankton acts a bio-control  
550 by changing the state of chaos to order.

## 551 Acknowledgements

552 The authors are grateful to the anonymous referees for their careful reading, valuable comments and  
553 helpful suggestions, which have contributed to improve the presentation of this work significantly. Au-  
554 thors are grateful to Prof. Guido Badino, DBIOS, University of Turin, Italy for his valuable suggestions.  
555 The research work of Saswati Biswas is supported by Council of Scientific and Industrial Research, Gov-  
556 ernment of India, New Delhi in the form of Senior Research Fellowship (Ref. No. 20/12/2015(ii)EU-V).

557 Pankaj Kumar Tiwari is thankful to University Grants Commissions, New Delhi, India for providing  
558 financial support in form of D. S. Kothari post-doctoral fellowship (No.F.4-2/2006 (BSR)/MA/17-  
559 18/0021). EV has been partially supported by the project “Metodi numerici e computazionali per le  
560 scienze applicate” of the Dipartimento di Matematica “Giuseppe Peano”.

## 561 References

- 562 1. Vaultot, D.: Phytoplankton. In: Encyclopedia of Life Sciences. Macmillan Publishers Ltd. 1–7 (2001)
- 563 2. Evans, C., Pond, D.W., Wilson, W.H.: Changes in *Emiliania huxleyi* fatty acid profiles during infection  
564 with *E. huxleyi* virus 86: physiological and ecological implications. *Aquat. Microb. Ecol.* **55**, 219–228 (2009)
- 565 3. Gilg, I.C. et al.: Differential gene expression is tied to photochemical efficiency reduction in virally infected  
566 *Emiliania huxleyi*. *Mar. Ecol. Prog. Ser.* **555**, 13–27 (2016)
- 567 4. Malitsky, S. et al.: Viral infection of the marine alga *Emiliania huxleyi* triggers lipidome remodeling and  
568 induces the production of highly saturated triacylglycerol. *New Phytol.* **210**(1), 88–96 (2016)
- 569 5. Rosenwasser, S. et al.: Rewiring host lipid metabolism by large viruses determines the fate of *Emiliania*  
570 *huxleyi*, a bloom-forming alga in the ocean. *Plant Cell tpc-114* (2014)
- 571 6. Suzuki, T., Yasuo, S.: Virus infection and lipid rafts. *Biol. Pharm. Bull.* **29**(8), 1538–1541 (2006)
- 572 7. Bratbak, G., Egge, J.K., Heldal, M.: Viral mortality of the marine alga *Emiliania huxleyi* (Haptophyceae)  
573 and termination of algal blooms. *Mar. Ecol. Prog. Ser.* 39–48 (1993)
- 574 8. Brussaard, C.P.D. et al.: Virus-like particles in a summer bloom of *Emiliania huxleyi* in the North Sea.  
575 *Aquat. Microb. Ecol.* **10**, 105–113 (1996)
- 576 9. Castberg, T. et al.: Microbial population dynamics and diversity during a bloom of the marine coccol-  
577 ithophorid *Emiliania huxleyi* (Haptophyta). *Mar. Ecol. Prog. Ser.* **221**, 39–46 (2001)
- 578 10. Nagasaki, K. et al.: Virus-like particles in *Heterosigina akashiwo* (Raphidophyceae): a possible red-tide  
579 disintegration mechanism. *Mar. Biol.* **119**(2), 307–312 (1994)
- 580 11. Jacquet, S. et al.: Flow cytometric analysis of an *Emiliana huxleyi* bloom terminated by viral infection.  
581 *Aquat. Microb. Ecol.* **27**, 111–124 (2002)
- 582 12. Costamagna, A. et al.: A model for the operations to render epidemic-free a hog farm infected by the  
583 Aujeszky disease. *Appl. Math. Nonlinear Sci.* **1**(1), 207–228 (2016)
- 584 13. Venturino, E.: Ecoepidemiology: a more comprehensive view of population interactions. *Math. Model. Nat.*  
585 *Phenom.* **11**(1), 49–90 (2016)
- 586 14. Samanta, S. et al.: Effect of enrichment on plankton dynamics where phytoplankton can be infected from  
587 free viruses. *Nonlinear Studies* **20**(2), 223–236 (2013)
- 588 15. Bairagi, N. et al.: Virus replication factor may be a controlling agent for obtaining disease-free system in  
589 a multi-species eco-epidemiological system. *J. Biol. Syst.* **13**(3), 245–259 (2005)
- 590 16. Evans, C., Wilson, W.H.: Preferential grazing of *Oxyrrhis marina* on virus infected *Emiliania huxleyi*.  
591 *Limnol. Oceanogr.* **53**, 2035–2040 (2008)

- 
- 592 17. Vermont, A. et al.: Virus infection of *Emiliana huxleyi* deters grazing by the copepod *Acartia tonsa*. J.  
593 Plankton Res. **38(5)**, 1194–1205 (2016)
- 594 18. Townsend, D.W. et al.: Blooms of the coccolithophore *Emiliana huxleyi* with respect to hydrography in  
595 the Gulf of Maine. Cont. Shelf Res. **14**, 979–1000 (1994)
- 596 19. Wilson, W.H. et al.: Isolation of viruses responsible for the demise of an *Emiliana huxleyi* bloom in the  
597 English Channel. J. Mar. Biol. Assoc. U.K. **82(3)**, 369–377 (2002)
- 598 20. Evans, C.: The influence of marine viruses on the production of dimethyl sulphide (DMS) and related  
599 compounds from *Emiliana huxleyi*. PhD Thesis, University of East Anglia (2005)
- 600 21. Evans, C. et al.: Viral infection of *Emiliana huxleyi* (Prymnesiophyceae) leads to elevated production of  
601 reactive oxygen species. J. Phycol. **42**, 1040–1047 (2006)
- 602 22. Poulet, S.A., Ouellet, G.: The role of amino acids in the chemosensory swarming and feeding of marine  
603 copepods. J. Plankton Res. **4**, 341–361 (1982)
- 604 23. Gill, C.W., Poulet, S.A.: Responses of copepods to dissolved free amino acids. Mar. Ecol. Prog. Ser. **43**,  
605 269–276 (1988)
- 606 24. Demott, W.R., Watson, M.D.: Remote detection of algae by copepods: responses to algal size, odors and  
607 motility. J. Plankton Res. **13**, 1203–1222 (1991)
- 608 25. Steinke, M., Stefels, J., Stamhuis, E.: Dimethyl sulfide triggers search behavior in copepods. Limnol.  
609 Oceanogr. **51**, 1925–1930 (2006)
- 610 26. Floge, S.A.: Virus infections of eukaryotic marine microbes, Electronic Theses and Dissertations. The  
611 University of Maine (2014)
- 612 27. Evans, C. et al.: The relative significance of viral lysis and microzooplankton grazing as pathways of dimethyl-  
613 sulfoniopropionate (DMSP) cleavage: an *Emiliana huxleyi* culture study. Limnol. Oceanogr. **52**, 1036–1045  
614 (2007)
- 615 28. Predators in the Plankton, Available at  
616 <http://oceans.mit.edu/news/featured-stories/predators-in-the-plankton.html>
- 617 29. Mukherjee, D.: Persistence in a prey-predator system with disease in the prey. J. Biol. Syst. **11(01)**,  
618 101–112 (2003)
- 619 30. Venturino, E.: Epidemics in predator-prey models: disease in the prey, In: Arino, O., Axelrod, D., Kim-  
620 mel, M., Langlais, M. (Eds.), Mathematical Population Dynamics: Analysis of Heterogeneity, **1**, 381–393  
621 (1995)
- 622 31. Chattopadhyay, J., Arino, O.: A predator-prey model with disease in the prey. Nonlinear Analysis **36**,  
623 747–766 (1999)
- 624 32. Hethcote, H.W. et al.: A predator-prey model with infected prey. Theor. Popul. Biol. **66(3)**, 259–268  
625 (2004)
- 626 33. Beretta, E., Kuang, Y.: Modeling and analysis of a marine bacteriophage infection. Math. Biosci. **149**,  
627 57–76 (1998)
- 628 34. Siekmann, I., Malchow, H., Venturino, E.: An extension of the Beretta-Kuang model of viral diseases.  
629 Math. Biosci. Eng. **5**, 549–565 (2008)
- 630 35. Hilker, F.M. et al.: Oscillations and waves in a virally infected plankton system Part II: Transition from  
631 lysogeny to lysis. Ecol. Compl. **3**, 200–208 (2006)

- 
- 632 36. Bhattacharyya, S., Bhattacharya, D.K.: Pest control through viral disease: mathematical modeling and  
633 analysis. *J. Theor. Biol.* **238**(1), 177–197 (2006)
- 634 37. Beltrami, E., Carroll, T.O.: Modeling the role of viral disease in recurrent phytoplankton blooms. *J. Math.*  
635 *Biol.* **32**, 857–863 (1994)
- 636 38. Gakkhar, S., Negi, K.: A mathematical model for viral infection in toxin producing phytoplankton and  
637 zooplankton system. *Appl. Math. Comp.* **179**, 301–313 (2006)
- 638 39. Chattopadhyay, J., Pal, S.: Viral infection on phytoplankton-zooplankton system: a mathematical model.  
639 *Ecol. Model.* **151**, 15–28 (2002)
- 640 40. Rhodes, C., Truscott, J., Martin, A.: Viral infection as a regulator of oceanic phytoplankton populations.  
641 *J. Mar. Syst.* **74**, 216–226 (2008)
- 642 41. Singh, B.K., Chattopadhyay, J., Sinha, S.: The role of virus infection in a simple phytoplankton-zooplankton  
643 system. *J. Theor. Biol.* **231**, 153–166 (2004)
- 644 42. Rhodes, C.J., Martin, A.P.: The influence of viral infection on a plankton ecosystem undergoing nutrient  
645 enrichment. *J. Theor. Biol.* **265**(3), 225–237 (2010)
- 646 43. May, R.M.: Chaos and the dynamics of biological populations. *Proc. R. Soc. Lond.* **413**, 27–44 (1987)
- 647 44. Godfray, H.C.J., Grenfell, B.T.: The continuing quest for chaos. *Trends Ecol. Evol.* **8**, 43–44 (1993)
- 648 45. Hastings, A. et al.: Chaos in ecology: is mother nature a strange attractor? *Annu. Rev. Ecol. Syst.* **24**,  
649 1–33 (1993)
- 650 46. Perry, J.N., Woiwod, I.P., Hanski, I.: Using response-surface methodology to detect chaos in ecological  
651 time series. *Oikos* **68**, 329–339 (1993)
- 652 47. Jørgensen, S.E.: The growth rate of zooplankton at the edge of chaos: ecological models. *J. Theor. Biol.*  
653 **175**, 13–21 (1995)
- 654 48. Hastings, A., Powell, T.: Chaos in three-species food chain. *Ecology* **72**, 896–903 (1991)
- 655 49. Chattopadhyay, J., Sarkar, R.R.: Chaos to order: preliminary experiments with a population dynamics  
656 models of three trophic levels. *Ecol. Model.* **163**, 45–50 (2003)
- 657 50. Peters, R.H.: The ecological implications of body size. Cambridge University Press, Cambridge (1983)
- 658 51. Mandal, S. et al.: Order to chaos and vice versa in an aquatic ecosystem. *Ecol. Model.* **197**, 498–504 (2006)
- 659 52. Chakraborty, S. et al.: The role of avoidance by zooplankton for survival and dominance of toxic phyto-  
660 plankton. *Ecol. Compl.* **11**, 144–153 (2012)
- 661 53. Holmes, J.C., Bethel, W.M.: Modification of intermediate host behavior by parasites, In: Canning, E.V.,  
662 Wright, C.A. (Eds.), Behavioral Aspects of Parasite Transmission. Suppl. I to *Zool. f. Linnean Soc.* **51**,  
663 123–149 (1972)
- 664 54. Lafferty, K.D.: Foraging on prey that are modified by parasites. *Am. Nat.* **140**, 854–867 (1992)
- 665 55. Hamilton, W.D., Axelrod, R., Tanese, R.: Sexual reproduction as an adaptation to resist parasite: a review.  
666 *Proc. Natl Acad. Sci. USA* **87**, 3566–3573 (1990)
- 667 56. Uhlig, G., Sahling, G.: Long-term studies on *Noctilucascintillans* in the German bight. *Neth. J. Sea Res.*  
668 **25**, 101–112 (1992)
- 669 57. Lakshmikantham, V., Leela, S., Martynuk, A.A.: Stability analysis of nonlinear systems. Marcel Dekker,  
670 Inc. New York/Basel (1989)

- 
- 671 58. Smith, H.L.: The Rosenzweig-MacArthur predator-prey model. [https://math.la.asu.edu/halsmith/](https://math.la.asu.edu/halsmith/Rosenzweig.pdf)  
672 [Rosenzweig.pdf](https://math.la.asu.edu/halsmith/Rosenzweig.pdf)
- 673 59. Li, Y., Muldowney, J.S.: On Bendixson's criterion, *J. Diff. Eqn.* **106**, 27–39 (1993)
- 674 60. Marino, S. et al.: A methodology for performing global uncertainty and sensitivity analysis in systems  
675 biology. *J. Theor. Biol.* **254(1)**, 178–196 (2008)
- 676 61. Rosenzweig, M.L.: Paradox of enrichment: destabilization of exploitation ecosystems in ecological time.  
677 *Science* **171**, 385 (1971)
- 678 62. Linhart, S.B. et al.: Avoidance of prey by captive coyotes punished with electric shock. In: Proceedings of  
679 the Vertebrate Pest Conference **7**, 302–330 (1976)
- 680 63. Lebedeva, L.P.: A model of the latitudinal distribution of the numbers of species of phytoplankton in the  
681 sea. *J. Cons. Int. Explor. Mer.* **34**, 341–350 (1972)
- 682 64. Jørgensen, S.E. et al.: Improved calibration of a eutrophication model by use of the size variation due to  
683 succession. *Ecol. Model.* **153**, 269–277 (2002)
- 684 65. Odum, H.T.: Self organization, transformity, and information. *Science* **242**, 1132–1139 (1988)
- 685 66. Kauffman, S.A.: Anti-chaos and adaptation. *Sci. Am.* **265(2)**, 78–84 (1991)